

INTRODUCTION

Sludge (biosolids), produced in large amounts at sewage treatment plants, is a potentially useful waste material that could find further application if properly treated. However, the presence of potentially dangerous pollutants, such as bacteria/viruses, pharmaceuticals, polychlorinated biphenyls and polycyclic aromatic hydrocarbons makes this problematic. Within the whole project, we describe a process through which useful tree planting substrates can be produced by i) composting the sludge to reduce pollutant content, ii) using the composted sewage sludge together with peat, bark or wood substrates, and iii) adding granulated glauconite as a significant natural source of potassium and biochar as a sorbent of high levels of atmospheric carbon and other nutrients as well as any remaining pollutants. We also describe methods for testing the safety (toxicity) of the resulting substrates and evaluate the economic costs of production and use. This contribution is objected to the evaluation of pharmaceuticals and industrial substances residues content in substrates based on treated sludge. Also a few examples of practical use are presented, as both forestry and arborist experiments has been set up recently on several research plots.

MATERIALS AND METHODS

For the purposes of whole project, three variants of substrates were prepared, when peat or crushed bark was mixed with sewage sludge. In this contribution, the average values of the substances content of all three substrates together are used for the brief comparison. The average values for comparison are calculated from values of following variants of substrates: (1) sludge + highmoor white peat (1:3), (2) sludge + crushed bark (1:3), (3) sludge + transition white peat (1:3). The evaluation is carried out for each project stage and sub-stage, where: IZ – 1st stage, state before composting, IK – 1st stage, first composting, IIK – 2nd stage – pouring with digestate, second composting. As part of the 3rd stage, the obtained substrates from the previous stages were finally mixed – 4P, and this mix was further enriched with peat – 5P (Table 1). The pharmaceuticals content was also detected in the biomass of lettuce (*Lactuca sativa* L.), which was grown in prepared substrates. Screening was performed according to valid methodologies (Brunetti et al. 2021, Golovko et al. 2016, Kodešová et al. 2023).

Table 1: Composting and sampling workflow

	1st stage	2nd stage	3rd stage
substrate (1)	1st composting	digestate 2nd composting	mix
substrate (2)	1st composting	digestate 2nd composting	mix
substrate (3)	1st composting	digestate 2nd composting	mix + peat
IZ	IK	IIK	4P
			5P

Table 2: The groups of analyzed pharmaceuticals and industrial substances

Substance group	Affect on organs and their systems, pharmacological affect and chemical composition	Analyzed substances
Industrial substances		1H-Benzotriazole (HOB), 1-Methyl-1H-Benzotriazole (MBE), 4,5-Methyl-1H-Benzotriazole, 2-Phenylbenzimidazol-5-sulfonic acid (PBA)
C-pharmaceuticals	Cardiovascular system	Atenolol, Amlodipine, Bisoprolol, Fenofibrate, Rosartan, Metoprolol, Metoprolol acid, Propranolol, Rosuvastatin, Sildenafil, Valsartan, Vasopressin
N-pharmaceuticals	Nervous system	Amphetamine, Caffeine, Carbamazepine and its metabolite CBZ 10,11-epoxide, CBZ 10,11-epoxide, CBZ 10,11-trans-dihydroxy 10,11-dihydroxy, Clonidine, Gabapentin, Lamotrigine, Mefenamic acid, N-desmethylnaloxonium, Nefazodone, O-desmethylnaloxonium, O-desmethylnaloxonium, Oxycodone, Oxycodone, Sertraline, Tramadol, Triazoline, Valproate
J-pharmaceuticals	Antibiotics, anti-infectives	Azithromycin, Clarithromycin, Clindamycin and its metabolite Clindamycin sulfide, Erythromycin, Nifedipine, Nifedipine, Sulfamethoxazole, Sulfapyridine, Trimethoprim
M-pharmaceuticals	Musculoskeletal system	Diclofenac
R-pharmaceuticals	Respiratory system	Cetirizine, Diphenhydramine, Fexofenadine
A-pharmaceuticals	Digestive system and metabolism	Loperamide

OBJECTIVE

The main objective of this contribution is to present the overall results of pharmaceuticals and industrial substances content in the substrates based on treated sewage sludge and to evaluate the gradual effect of composting on reducing the pharmaceutical content from a broader perspective, as this study was performed as a crucial part of the whole project to describe the toxicity and safety of resulting substrates. Finally we would like to present a two examples of substrate use in forest nurseries and for the arboricultural plantings.

RESULTS

Occurrence screening was performed for 51 substances in total – three benzotriazoles, one UV filter, 38 pharmaceuticals and nine of their metabolites, these substances were divided into a total of seven groups – 1 collective group for industrial substances and six groups of pharmaceuticals according to their effectiveness on organs, organ systems, pharmacological affect and chemical composition – medicals classification according to WHO (ATC/DDD Index 2023), (Table 2). Before composting, the highest contents were found in the cases of C-pharmaceuticals, M-pharmaceuticals and R-pharmaceuticals (IZ). After the first composting (IK), a significant reduction in the contents of most of the analysed pharmaceuticals and industrial substances was observed (by up to 50% on average), whereas in most cases the content further decreased with the second composting (IIK). However after the second the content reduction was not so significant, especially in the case of M-pharmaceuticals, that slightly increased backwards. Comparing the mixed substrates developed during the 3rd stage, we can say that substrate with added peat contains on average twice as many substances as substrate prepared only as a simple mixture of those premixes from previous stage. Excepting A-pharmaceuticals, the amounts of substances in substrate with peat (5P) are comparable with the values after the second composting (IIK). Simple mixed substrate (4P) shows the lowest values of substances content (Table 3, Figure 1). Tests in the lettuce biomass detected a significant amount of J-pharmaceuticals absorbed from the substrate after the second composting, in the case of industrial substances, R-pharmaceuticals and A-pharmaceuticals the amount also slightly increased. Compared to that, the amount of C-pharmaceuticals, M-pharmaceuticals and N-pharmaceuticals decreased in lettuce biomass. Interesting issue is that plants grown in the mixed substrates tended to cumulate industrial substances and J-pharmaceuticals in both substrate mixtures, M-pharmaceuticals in the simple mixture (4P) and C-pharmaceuticals, R-pharmaceuticals and A-pharmaceuticals grown in the mixed substrate with added peat (5P).

Table 3: The amount of pharmaceuticals and industrial substances content in premixed substrates

	[ng.g ⁻¹]					[%] of the default (column IZ)				
Substrates	IZ	IK	IIK	4P	5P	IK	IIK	4P	5P	
Industrial substances	69,58	39,10	5,50	1,44	5,29	56,20%	7,91%	2,07%	7,60%	
C-pharmaceuticals	204,62	12,58	9,12	3,57	8,37	6,15%	4,46%	1,74%	4,09%	
N-pharmaceuticals	77,79	19,70	9,54	4,21	8,77	25,32%	12,27%	5,41%	11,27%	
J-pharmaceuticals	7,97	4,98	2,56	1,38	2,13	62,51%	32,13%	17,32%	26,74%	
M-pharmaceuticals	113,33	5,00	7,63	5,60	8,20	4,41%	6,74%	4,94%	7,24%	
R-pharmaceuticals	96,00	25,49	8,71	2,79	8,43	26,55%	9,07%	2,91%	8,78%	
A-pharmaceuticals	7,43	3,47	1,38	1,10	1,90	46,64%	18,52%	14,80%	25,56%	
		decrease								
		increase								

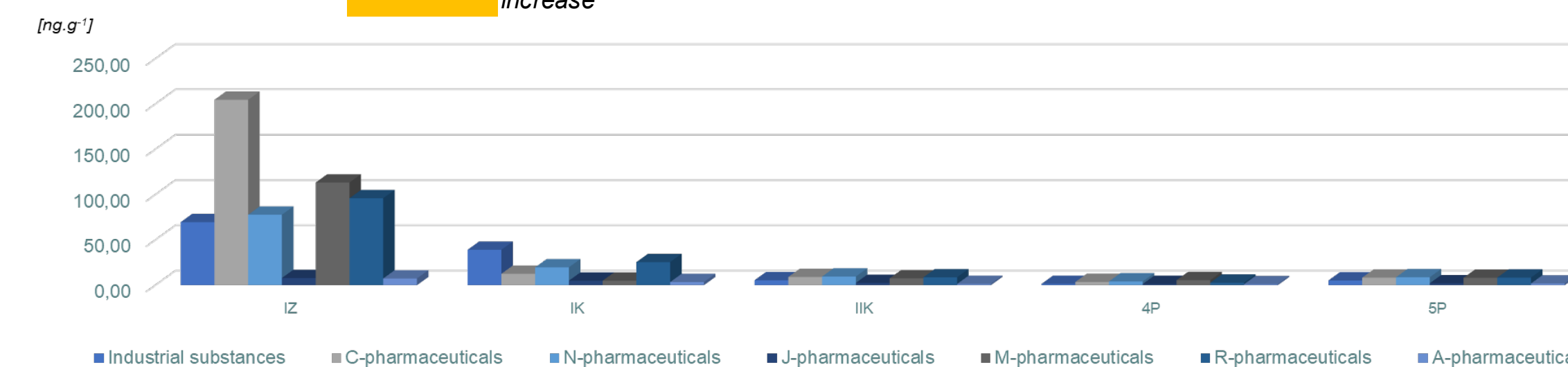


Figure 1: The amount of pharmaceuticals and industrial substances content in premixed substrates

Table 4: The amount of pharmaceuticals and industrial substances content in lettuce biomass

	[ng.g ⁻¹]				[%] of the default (column IK)		
Lettuce biomass	IK	IIK	4P	5P	IIK	4P	5P
Industrial substances	7,79	7,98	12,84	14,00	102,48%	164,83%	179,72%
C-pharmaceuticals	3,04	2,88	2,21	6,68	94,74%	72,70%	219,74%
N-pharmaceuticals	12,21	8,52	10,31	9,40	69,75%	84,44%	76,99%
J-pharmaceuticals	2,00	2,69	2,86	3,17	134,33%	143,00%	158,50%
M-pharmaceuticals	4,33	4,00	5,00	4,00	92,31%	115,38%	92,31%
R-pharmaceuticals	2,41	2,47	2,18	2,63	102,21%	90,33%	108,98%
A-pharmaceuticals	1,67	1,73	1,50	1,80	104,00%	90,00%	108,00%
		decrease					
		increase					

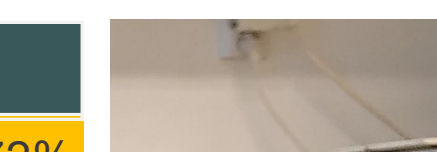


Figure 2: *Lactuca sativa*

Figure 2: *Lactuca sativa* L.

CONCLUSIONS

In conclusion, it can be stated that the most residues of C-pharmaceuticals affecting the cardiovascular system were detected in sewage sludge, which corresponds to the fact that diseases of the heart and blood vessels are the most common diseases in the Czech Republic. With the proposed technology, when treated sewage sludge is added to the substrate and then twice composted, there is a significant reduction of all detected pharmaceuticals and industrial substances. Substrate can further be used as relatively safe for growing non eatable plants (only), as currently most of the stabilized sludge is exported to farmland, and thus potential pollutants enter the food chain. The substrate use for growing seedlings in forest nurseries and for arboricultural plantings is currently being tested on several research plots (Figure 3).

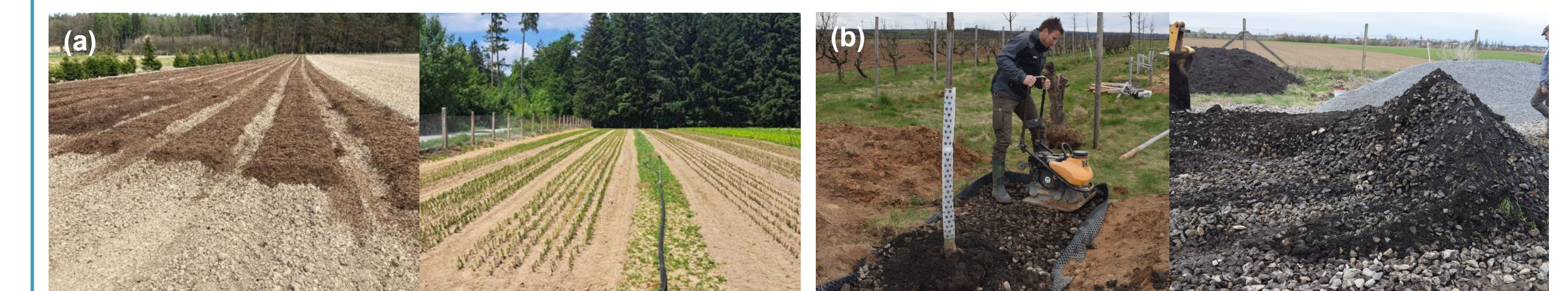


Figure 3: (a) Substrate ready to be plowed and Norway spruce seedlings, (b) planting the lindens in a pit filled with premixed substrate

ACKNOWLEDGEMENTS

This research was performed within the project CZ.01.1.02/0.0/0.0/20_321/0024778 „Optimalizace úpravy a zpracování kalů z čistíren odpadních vod při výrobě pěstebních substrátů a jejich bezpečné využití“ funded by Ministry of Industry and Trade and European Fund for Regional Development.

Brunetti, G., Kodesova, R., Svecova, H., Fer, M., Nikodem, A., Klement, A., Grabic, R., & Simunek, J. (2021). On the Use of Mechanistic Soil-Plant Uptake Models: A Comprehensive Experimental and Numerical Analysis on the Translocation of Carbamazepine in Green Pea Plants. *Environmental Science and Technology*, 55(5), 2991–3000. <https://doi.org/10.1021/acs.est.0c07420>
Golovko, O., Koba, O., Kodešová, R., Fedorova, G., Kumar, V., & Grabic, R. (2016). Development of fast and robust multiresidual LC-MS/MS method for determination of pharmaceuticals in soils. *Environmental Science and Pollution Research*, 23(14), 14068–14077. <https://doi.org/10.1007/s11356-016-6487-6>
Kodešová, R., Fedorova, G., Kodeš, V., Kočánek, M., Rieznýk, O., Fer, M., Svecova, H., Klement, A., Bofik, A., Nikodem, A., & Grabic, R. (2023). Assessment of potential mobility of selected micropollutants in agricultural soils of the Czech Republic using their sorption predicted from soil properties. *Science of the Total Environment*, 865(December 2022). <https://doi.org/10.1016/j.scitotenv.2022.161174>
ATC/DDD Index 2023 https://www.whooc.no/atc_ddd_index/



INTRODUCTION

During commercial seed production, vegetable seeds may become infected with various bacterial phytopathogens after systemic colonization of plants upon leaf infection. The species *Brassica oleracea* included plants grown and consumed worldwide. Black rot is one of the most important diseases that affect *B. oleracea*, reducing the quality of crops and causing great economic losses. This disease is caused by Gram-negative bacteria *Xanthomonas campestris* pv. *campestris* (Xcc). Moreover, other representatives of the genus *Xanthomonas* can incite leaf-spot disease.

AIM

Quick detection of potentially presented bacteria pathogens on seed surface of four Brassica species - cabbage, kale, kohlrabi and broccoli.

MATERIALS AND METHODS

The eluate from seeds surface by Tris-EDTA buffer was cultivated on nutrition agar medium (0.5% peptone, 0.3% beef extract, 1.5% agar and 20% glucose) in Petri dishes at 30 °C for 48 hours. Bacteria cell suspension (diluted bacteria colony in Tris-EDTA buffer) was used directly as template in PCR detection. We tested universal 16S rRNA primers as well as specific primers for identification of *X. campestris* pv. *campestris* (Xcc), *X. perforans* (Xp), *X. euvesicatoria* (Xe), *X. gardneri* (Xg) and *X. vesicatoria* (Xv). The PCR was performed using KAPA2G Fast HotStart Ready Mix (2x), forward and reverse primers (each 10 µM), template DNA. PCR assays were performed with BioRad thermocycler. Reactions were run for 35 cycles, each consisting of 15 s at 95 °C, 15 s at 54-75 °C (different annealing temperature for each primer pair), and 15 s at 72 °C, with initial denaturation of 3 min at 95 °C and final extension of 15 min at 72 °C. PCR products were separated using horizontal electrophoresis system (Major Science) on a 1% agarose gel and visualised by UV-transilluminator (SmartView Pro 1100).

RESULTS

- All tested samples were positive in PCR with bacterial 16S rRNA.
- Among the 5 tested specific primers, we confirmed only the presence of *X. euvesicatoria* in all vegetable samples.

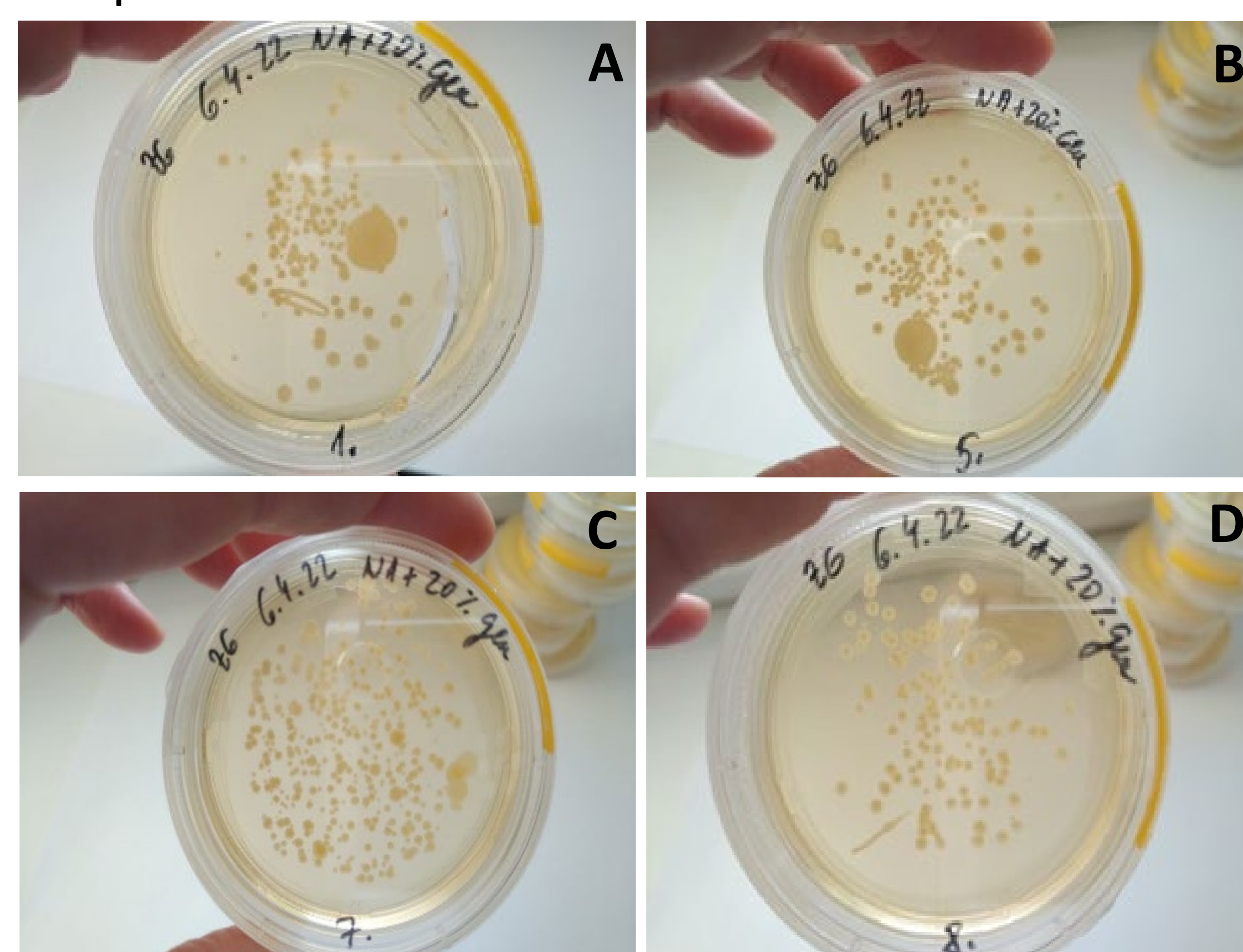


Fig. 1. Bacteria colonies grown on nutrition agar media with 20% glucose at 30 °C for 48 h (A – cabbage, B – kale, C – kohlrabi, D – broccoli).

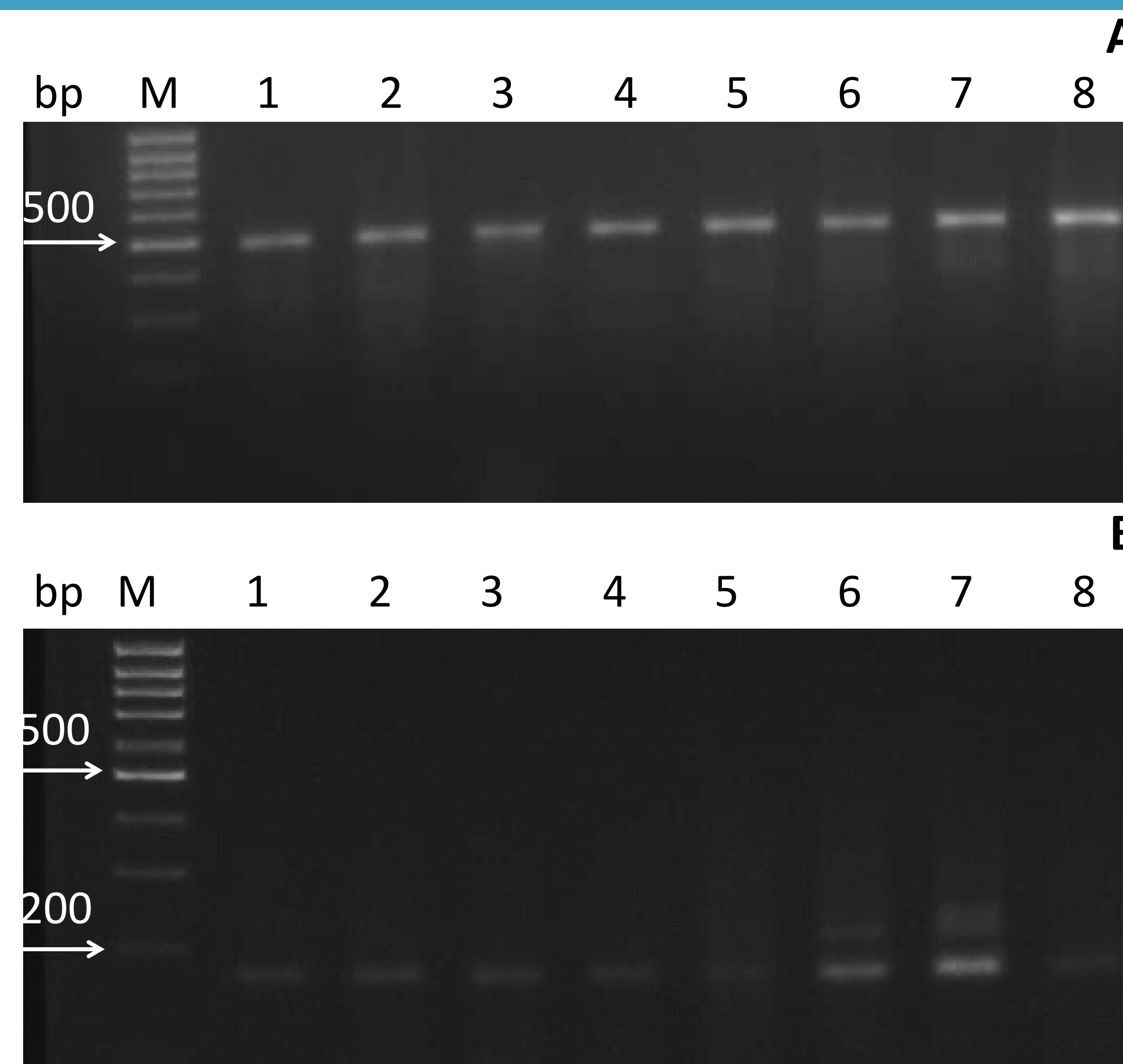


Fig. 2. Amplification of 500 bp DNA fragment of 16S rRNA (A) and 173 bp DNA fragment of the *hrp* gene from *X. euvesicatoria* (B) detected on the seeds surface of cabbage (1 – cv. Madison, 2 – cv. Capitot, 3 – cv. Kalibos, 4 – cv. Avak F1), kale (5,6 – cv. Scarlet), kohlrabi (7 – cv. Kref F1) and broccoli (8 – cv. Limba).

CONCLUSIONS

We confirmed the presence of bacterial microorganisms on the seed surface of all tested Brassica species using 16S rRNA primers. Among tested Xanthomonads, we found the presence of only *X. euvesicatoria* on seeds of kale, kohlrabi, broccoli as well as cabbage.

ACKNOWLEDGEMENTS

This work was supported by the grant INTERREG 304011X035.

GENETIC DIVERSITY OF THE *GANODERMA* SPECIES IN CENTRAL EUROPE

TERÉZIA BECK^{1*}, MARTIN ŠEBESTA², KATEŘINA NÁPLAVOVÁ³, PETER PRISTAŠ⁴

¹Department of Biology, Ecology and Environment, Faculty of Natural Sciences, Matej Bel University, Tajovskeho 40, 974 01 Banská Bystrica, Slovakia

²T-Mapy s.r.o., Dvojkrizna 49, 821 06 Bratislava, Slovakia

³Department of Biology and Ecology, Faculty of Science, University of Ostrava, Chittussiho 10, 710 00 Ostrava, Czech Republic

⁴Institute of Biology and Ecology, Pavol Josef Safarik University in Kosice, Srobarova 2, 041 01 Kosice, Slovakia

INTRODUCTION

Ganoderma (Basidiomycota) is a cosmopolitan wood-decay polypore causing white rot of a wide range of woody plants (1,2). It plays an important role in the process of wood decomposition in forest ecosystems, but it is also known as a dangerous phytopathogen (3). *Ganoderma* species were classified primarily on the basis of morphological features, such as an appearance of pileus surface (dull or laccate, resinous deposits), colour of the context, presence of the stipe, and shape, size and ornamentation of the basidiospores (2, 4-7). However, many taxonomy confusions have resulted from the great variability in the macroscopic characters of the *Ganoderma* basidiomata (3). As a consequence of several molecular phylogenetic studies, an unexpectedly high level of species diversity in *Ganoderma* has been uncovered worldwide (3) and molecular analyses have been shown to be a valuable tool in their current taxonomy (8). Currently, there are 492 names in the Index Fungorum (9) and 535 records of taxa (482 with status legitimate) in MycoBank (10). Up to now, 181 species are taxonomically accepted in *Ganoderma* (3), most of them originate from the tropics (11, 12). Only 7 species naturally occur in Central Europe: *Ganoderma applanatum* (Pers.) Pat., *G. adspersum* (Schulzer) Donk, *G. pfeifferi* Bres., *G. resinaceum* Boud., *G. carnosum* Pat., *G. lucidum* (Curtis) P. Karst., *G. valesiacum* Boud. (2, 6, 13, 14). Although many molecular studies have been conducted within the genus, especially within *G. lucidum* complex (15, 16), available data from Central Europe are rare.

AIM

The aim of the present study was to analyze both interspecific and intraspecific genetic variability in *Ganoderma* genus using molecular methods based on European ITS (internal transcribed spacer) sequences. In order to analyze the genetic diversity observed at the ITS level in more detail, partial translation elongation factor 1- α (tef1- α) sequences were obtained and analyzed.



Ganoderma adspersum



Ganoderma lucidum

ACKNOWLEDGEMENTS

This work was funded by KEGA Grant No. 014UMB-4/2023 and VEGA Grant No. 1/0564/21 and by the ITMS Research & Development Operational Programme; ERDF, Grant/Award No. 26210120024.

MATERIALS AND METHODS

Fungal Collections

- 75 *Ganoderma* basidiocarps were collected during the years 2015-2018 in Slovakia, Czech Republic (Moravia) and in one place in northern Hungary (Fig. 1)

DNA Isolation

- 2X CTAB lysis solution (2 % w/v CTAB, 100 mM Tris-HCl, 20 mM EDTA, 1.4 M NaCl, pH 8.0) was used, the DNA was extracted using chloroform and precipitated with a 0.7-volume of isopropyl alcohol

PCR amplification and Sanger Sequencing

- for amplification of ITS and tef1- α molecular markers PCR primers and conditions were used as already described Beck et al. 2020 (17) and Náplavová et al. 2020 (18)

- the PCR products were purified using ExoSAP-IT (Affymetrix, Inc., Cleveland, Ohio USA), then sequenced in both directions using the same primers as for PCR at SEQme s.r.o. (Dobříš, Czech Republic).

Phylogenetic analyses

- the assembled sequences were aligned using clustalw algorithm and phylogenetic tree was constructed using Neighbor-Joining method. The reliability of estimated phylogenetic tree was evaluated using bootstrapping with 1000 repetition. For all phylogenetic analysis MEGA software version 7 was used (19). The similarity of aligned sequences was visualized using Bioedit software.

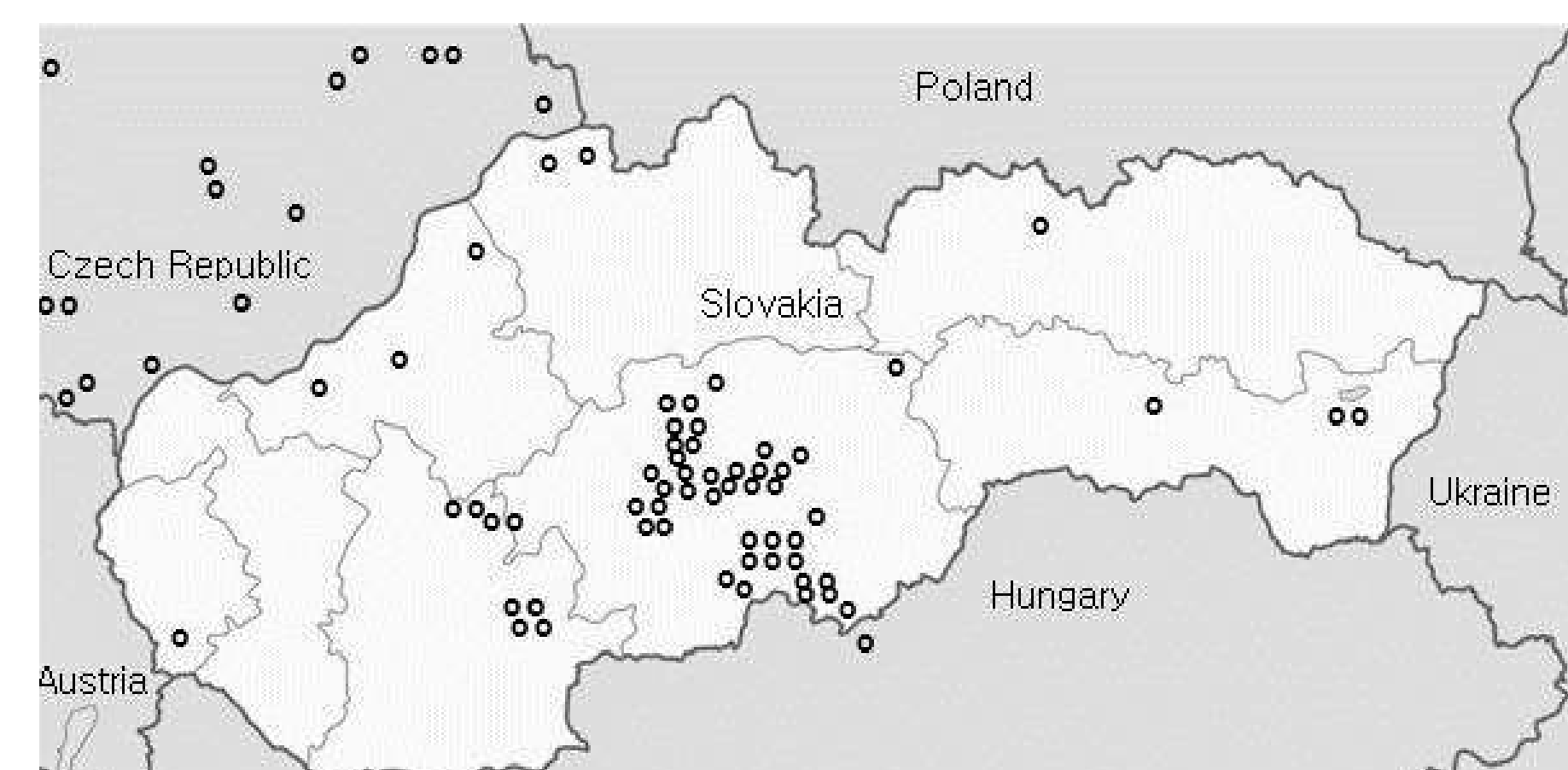


Fig. 1 Schematic map illustrating the spatial distribution of our *Ganoderma* collections in Central Europe

RESULTS

The species/specimens recognized in the study, their geographical locations in Central Europe, their hosts and ITS GenBank accessions numbers are given in Table 1:

Species/specimen No.	Geographical origin	Host	GenBank accession No.	Host	Geographical origin	Host	GenBank accession No.
<i>Ganoderma applanatum</i>	Slovakia	Fagus sylvatica	MAK12171	SL	Czech Republic	Quercus sp.	MAK12120
FRS	Slovakia	Fagus sylvatica	MAK12121	SL	Slovakia	Quercus sp.	MAK12121
MA115	Slovakia	Fagus sylvatica	MAK12122	SL	Slovakia	Quercus sp.	MAK12122
SL	Czech Republic	unknown	MAK12142	SL	Czech Republic	unknown	MAK12142
MA116	Slovakia	Fagus sylvatica	MAK12143	SL	Slovakia	unknown	MAK12143
MA117	Slovakia	Fagus sylvatica	MAK12144	SL	Slovakia	unknown	MAK12144
CA009ND	Slovakia	Fagus sylvatica	MAK12145	SL	Slovakia	unknown	MAK12145
BR109P	Slovakia	unknown	MAK12146	SL	Czech Republic	Pinus nigra	MAK12146
BR109P	Slovakia	unknown	MAK12147	SL	Czech Republic	Pinus nigra	MAK12147
BR109P	Slovakia	unknown	MAK12148	SL	Czech Republic	Pinus nigra	MAK12148
BR109P	Slovakia	unknown	MAK12149	SL	Czech Republic	Pinus nigra	MAK12149
BR109P	Slovakia	unknown	MAK12150	SL	Czech Republic	Pinus nigra	MAK12150
BR109P	Slovakia	unknown	MAK12151	SL	Czech Republic	Pinus nigra	MAK12151
BR109P	Slovakia	unknown	MAK12152	SL	Czech Republic	Pinus nigra	MAK12152
BR109P	Slovakia	unknown	MAK12153	SL	Czech Republic	Pinus nigra	MAK12153
BR109P	Slovakia	unknown	MAK12154	SL	Czech Republic	Pinus nigra	MAK12154
BR109P	Slovakia	unknown	MAK12155	SL	Czech Republic	Pinus nigra	MAK12155
BR109P	Slovakia	unknown	MAK12156	SL	Czech Republic	Pinus nigra	MAK12156
BR109P	Slovakia	unknown	MAK12157	SL	Czech Republic	Pinus nigra	MAK12157
BR109P	Slovakia	unknown	MAK12158	SL	Czech Republic	Pinus nigra	MAK12158
BR109P	Slovakia	unknown	MAK12159	SL	Czech Republic	Pinus nigra	MAK12159
BR109P	Slovakia	unknown	MAK12160	SL	Czech Republic	Pinus nigra	MAK12160
BR109P	Slovakia	unknown	MAK12161	SL	Czech Republic	Pinus nigra	MAK12161
BR109P	Slovakia	unknown	MAK12162	SL	Czech Republic	Pinus nigra	MAK12162
BR109P	Slovakia	unknown	MAK12163	SL	Czech Republic	Pinus nigra	MAK12163
BR109P	Slovakia	unknown	MAK12164	SL	Czech Republic	Pinus nigra	MAK12164
BR109P	Slovakia	unknown	MAK12165	SL	Czech Republic	Pinus nigra	MAK12165
BR109P	Slovakia	unknown	MAK12166	SL	Czech Republic	Pinus nigra	MAK12166
BR109P	Slovakia	unknown	MAK12167	SL	Czech Republic	Pinus nigra	MAK12167
BR109P	Slovakia	unknown	MAK12168	SL	Czech Republic	Pinus nigra	MAK12168
BR109P	Slovakia	unknown	MAK12169	SL	Czech Republic	Pinus nigra	MAK12169
BR109P	Slovakia	unknown	MAK12170	SL	Czech Republic	Pinus nigra	MAK12170
BR109P	Slovakia	unknown	MAK12171	SL	Czech Republic	Pinus nigra	MAK12171
BR109P	Slovakia	unknown	MAK12172	SL	Czech Republic	Pinus nigra	MAK12172
BR109P	Slovakia	unknown	MAK12173	SL	Czech Republic	Pinus nigra	MAK12173
BR109P	Slovakia	unknown	MAK12174	SL	Czech Republic	Pinus nigra	MAK12174
BR109P	Slovakia	unknown	MAK12175	SL	Czech Republic	Pinus nigra	MAK12175
BR109P	Slovakia	unknown	MAK12176	SL	Czech Republic	Pinus nigra	MAK12176
BR109P	Slovakia	unknown	MAK12177	SL	Czech Republic	Pinus nigra	MAK12177
BR109P	Slovakia	unknown	MAK12178	SL	Czech Republic	Pinus nigra	MAK12178
BR109P	Slovakia	unknown	MAK12179	SL	Czech Republic	Pinus nigra	MAK12179
BR109P	Slovakia	unknown	MAK12180	SL	Czech Republic	Pinus nigra	MAK12180
BR109P	Slovakia	unknown	MAK12181	SL	Czech Republic	Pinus nigra	MAK12181
BR109P	Slovakia	unknown	MAK12182	SL	Czech Republic	Pinus nigra	MAK12182
BR109P	Slovakia	unknown	MAK12183	SL	Czech Republic	Pinus nigra	MAK12183
BR109P	Slovakia	unknown	MAK12184	SL	Czech Republic	Pinus nigra	MAK12184
BR109P	Slovakia	unknown	MAK12185	SL	Czech Republic	Pinus nigra	MAK12185
BR109P	Slovakia	unknown	MAK12186	SL	Czech Republic	Pinus nigra	MAK12186
BR109P	Slovakia	unknown	MAK12187	SL	Czech Republic	Pinus nigra	MAK12187
BR109P	Slovakia	unknown	MAK12188	SL	Czech Republic	Pinus nigra	MAK12188
BR109P	Slovakia	unknown	MAK12189	SL	Czech Republic	Pinus nigra	MAK12189
BR109P	Slovakia	unknown	MAK12190	SL	Czech Republic	Pinus nigra	MAK12190
BR109P	Slovakia	unknown	MAK12191	SL	Czech Republic	Pinus nigra	MAK12191
BR109P	Slovakia	unknown	MAK12192	SL	Czech Republic	Pinus nigra	MAK12192
BR109P	Slovakia	unknown	MAK12193	SL	Czech Republic	Pinus nigra	MAK12193
BR109P	Slovakia	unknown	MAK12194	SL	Czech Republic	Pinus nigra	MAK12194
BR109P	Slovakia	unknown	MAK12195	SL	Czech Republic	Pinus nigra	MAK12195
BR109P	Slovakia	unknown	MAK12196	SL	Czech Republic	Pinus nigra	MAK12196
BR109P	Slovakia	unknown	MAK12197	SL	Czech Republic	Pinus nigra	MAK12197
BR109P	Slovakia	unknown	MAK12198	SL	Czech Republic	Pinus nigra	MAK12198
BR109P	Slovakia	unknown	MAK12199	SL	Czech Republic	Pinus nigra	MAK12199
BR109P	Slovakia	unknown	MAK12200	SL	Czech Republic	Pinus nigra	MAK12200

75 *Ganoderma* basidiocarps were divided into 6 clades according to phylogenetic analysis of ITS sequences: *Ganoderma applanatum*, *G. adspersum*, *G. resinaceum*, *G. pfeifferi*, *G. lucidum*, *G. carnosum* (Fig. 2). ITS sequences showed no close similarity of morphologically similar taxa *G. applanatum* and *G. adspersum*. Very low genetic diversity was observed between *G. lucidum* and *G. carnosum* clades. Significant intra-species genetic diversity was observed in *G. resinaceum* clade and, probably, the existence of 2 genotypes. Intraspecific variability was also confirmed by the analysis of tef1- α marker (Fig. 3). The observed diversity between 2 *G. resinaceum* genotypes was 0.0304 base substitutions per site, two times higher than diversity between *G. lucidum* and *G. carnosum* clades (0.016).

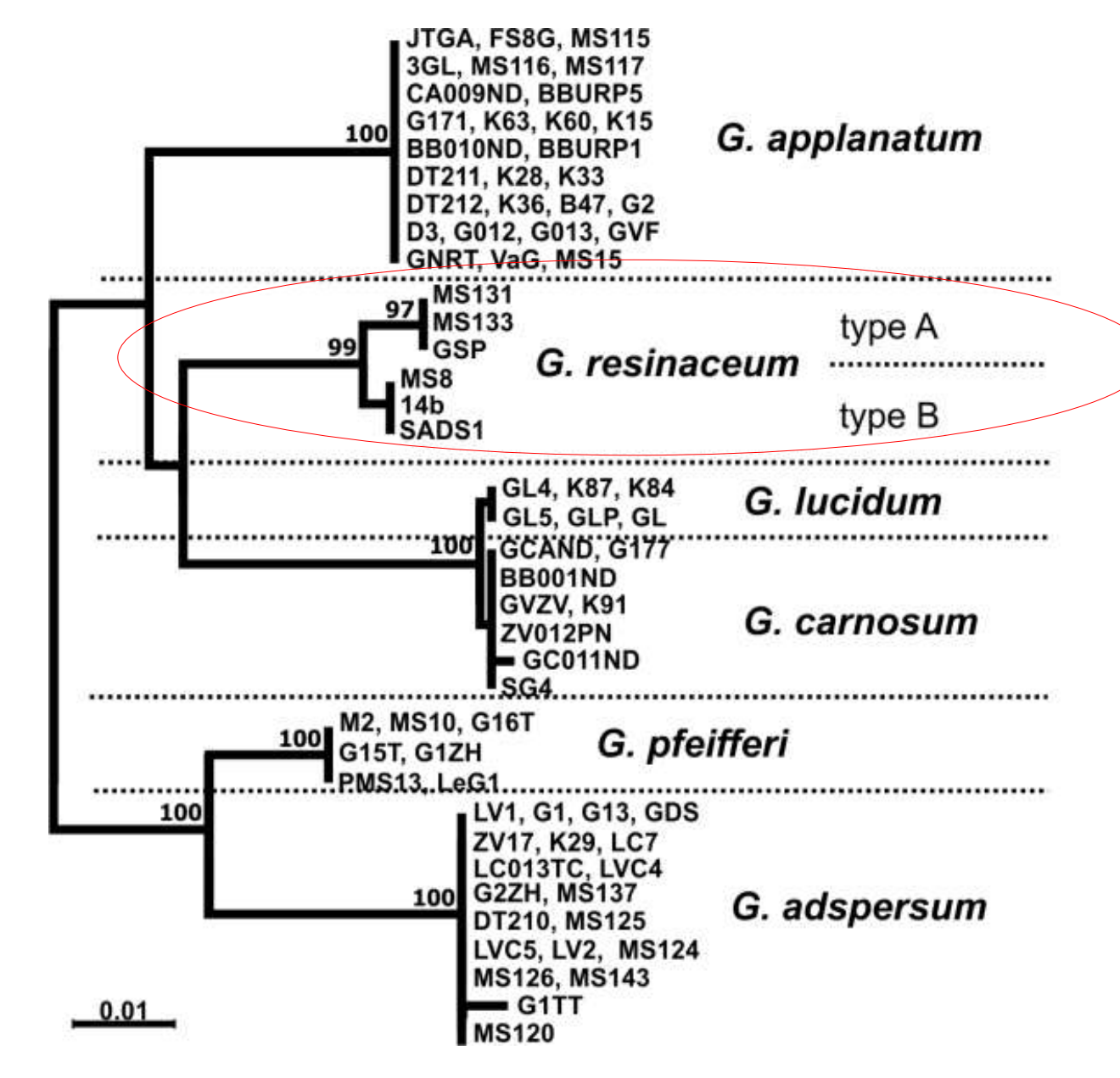


Fig. 2 Unrooted phylogenetic tree documenting the relatedness among Central European collections of *Ganoderma* spp.

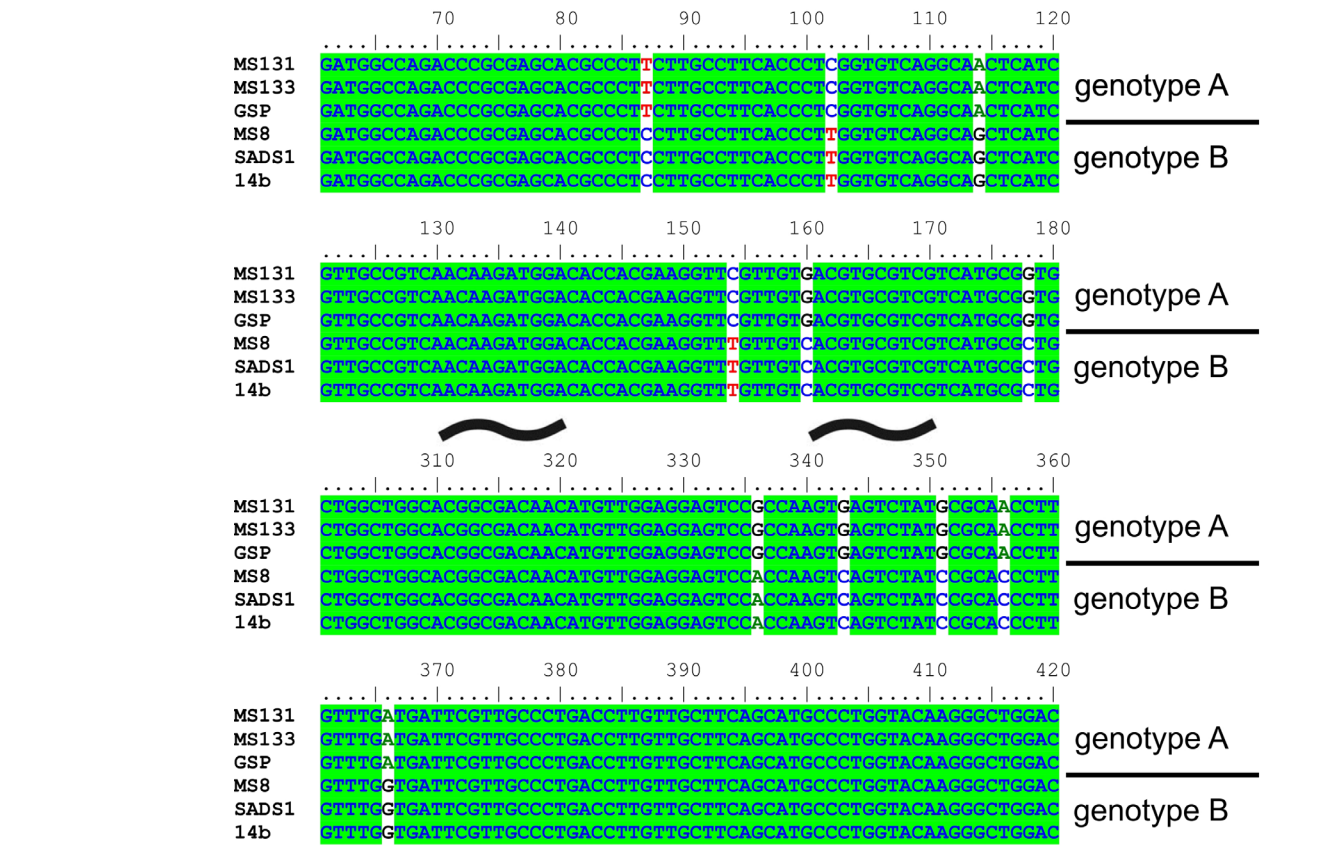


Fig. 3 Comparison of aligned tef1- α sequences of *G. resinaceum* genotypes A and B.

REFERENCES

- Schwarze FWMR, Ferner D. 2003 – *Ganoderma* on trees – differentiation of species and studies of invasiveness. Arboricultural Journal: The International Journal of Urban Forestry 27, 59–77.
- Ryvarden L, Melo I. 2014 – Poroid fungi of Europe. Fungiflora, Oslo.
- He J, Han X, Luo ZL, Li EX, Tang SM, Luo HM, Niu KY, Su XJ, Li SH. 2022 – Species diversity of *Ganoderma* (Ganodermataceae, Polyporales) with three new species and a key to *Ganoderma* in Yunnan Province, China. Frontiers in Microbiology 13, 1035434.
- Breitenbach J, Kranzlin F. 1986 – Fungi of Switzerland, Non gilled fungi, 2nd edn. Mykologia Verlag, Lucerne.
- Gilbertson RL, Ryvarden L. 1987 – North American polypores, 2nd edn. Fungiflora, Oslo.
- Bernicchia A. 2005 – Polyporaceae s.l., Fungi Europaei. Massimo Candusso, Alasio.
- Torres-Torres MB, Dávalos LG. 2012 – The morphology of *Ganoderma* species with a laccate surface. Mycotaxon 119, 201–216.
- Papp V. 2019 – Global Diversity of the Genus *Ganoderma*. In: Sridhar KR, Deshmukh SK (eds) Advances in Macrofungi. Diversity, Ecology and Biotechnology. CRC Press, Boca Raton, 10–33
- Cooper J, Kirk P. 2023 – CABI Bioscience Database, Landscape Research, Index Fungorum Database. <http://www.indexfungorum.org/Names/Names.asp> (accessed 01 September 2023).
- Robert V, Stegehuis G, Stalpers J. 2005 – The MycoBank engine and related databases. <https://www.Mycobank.org/> (accessed 01 September 2023).
- Moncalvo JM, Wang HH, Hseu RS. 1995 – Phylogenetic relationships in *Ganoderma* inferred from the internal transcribed spacers and 25S ribosomal DNA sequences. Mycologia 87, 223–238.
- Richter C, Wittstein K, Kirk PM, Stadler M. 2015 – An assessment of the taxonomy and chemotaxonomy of *Ganoderma*. Fungal Diversity 71, 1–15.
- Kotlíba F. 1984 – Zeměpisné rozšíření a ekologie chorošů (Polyporales s.l.) v Československu. Academia, Praha.
- Sokół S. 2000 – Ganodermataceae Polski : Taksonomia, ekologia i rozmieszczenie. Wydawnictwo Uniwersytetu Śląskiego, Katowice.
- Zhou LW, Cao Y, Wu SH, Vlasák J, Li DW, Dai YCH. 2015 – Global diversity of the *Ganoderma lucidum* complex (Ganodermataceae, Polyporales) inferred from morphology and multilocus phylogeny. Phytochemistry 114, 7–15.
- Xing JH, Song J, Decock C, Cui BK. 2016 – Morphological characters and phylogenetic analysis reveal a new species within the *Ganoderma lucidum* complex from South Africa. Phytotaxa 266, 115–124.
- Beck T, Gáperová S, Gáper J, Náplavová K, Šebesta M, Kisková J, Pristaš P. 2020 – Genetic (non)-homogeneity of the bracket fungi of the genus *Ganoderma* (Basidiomycota) in Central Europe. Mycosphere 11, 225–238.
- Náplavová K, Beck T, Pristaš P, Gáperová S, Šebesta M, Píknová M, Gáper J. 2020 – Molecular Data Reveal Unrecognized Diversity in the European *Ganoderma resinaceum*. Forests 11, 850.
- Kumar S, Stecher G, Tamura K. 2016 – MEGA7: Molecular Evolutionary Genetics Analysis version 7.0 for bigger datasets. Molecular Biology and Evolution 33, 1870–1874.



INTRODUCTION

Terpenes have antimicrobial, antioxidant, and other biological effects, which influence the use of many plants in traditional medicine, in the food and cosmetic industry. Plants produce terpenes that occur in essential oils produced in glandular secretory cells.

A unique terpene is caryophyllene, which occurs in four structural forms such as α -humulene, β -caryophyllene, isocaryophyllene and caryophyllene oxide. Plants mostly contain all structural forms, mainly β -caryophyllene and α -humulene dominate.

MATERIALS AND METHODS

Bacterial strains: *Escherichia coli* CCM 3954, *Micrococcus luteus* DSM 1790 and *Staphylococcus aureus* CCM 4223

Essential oils: Clove, lavender, oregano and sage

Pure substances: α -Humulene, β -caryophyllene, caryophyllene oxide

Preparation of the inoculum: The overnight cultures were diluted in culture medium and adjusted to a final concentration of 5×10^5 CFU/ml.

Methodology: Microdilution method; disk diffusion method

AIM

The aim of this work was to characterize the antibacterial potential of selected essential oils, clove, lavender, oregano and sage, containing caryophyllene and its structural forms against *Escherichia coli* CCM 3954, *Micrococcus luteus* DSM 1790 and *Staphylococcus aureus* CCM 4223.

RESULTS

Tab 1. Results of microdilution method

Essential oils and pure substances	<i>E. coli</i>	<i>M. luteus</i>	<i>S. aureus</i>
	MIC [μ l/ml]		
clove	≤ 1	≤ 1	≤ 1
lavender	2	4	≤ 1
oregano	≤ 1	≤ 1	≤ 1
sage	4	8	≤ 1
β -caryophyllene	512	512	256
α -humulene	512	512	32
caryophyllene oxide	>512	>512	>512

Tab 2. Content of structural forms of caryophyllene

Essential oil	clove	lavender	oregano	sage
β -caryophyllene	6,67 %	1,33 %	1,89 %	3,04 %
α -humulene	0,75 %	0,15 %	1,06 %	0,94 %

Results of disk diffusion method:

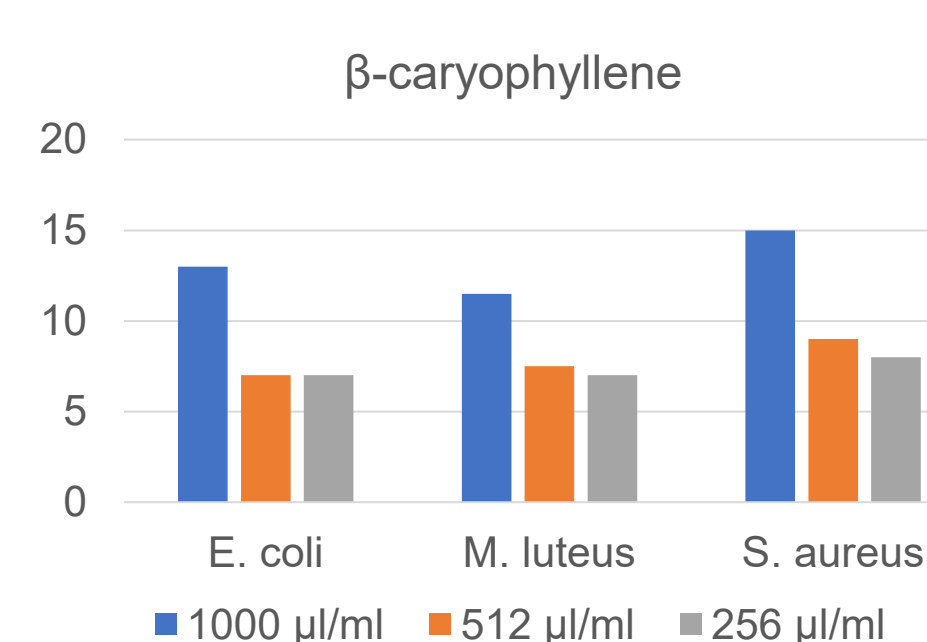


Fig. 1 Inhibition zones [mm] of β -caryophyllene

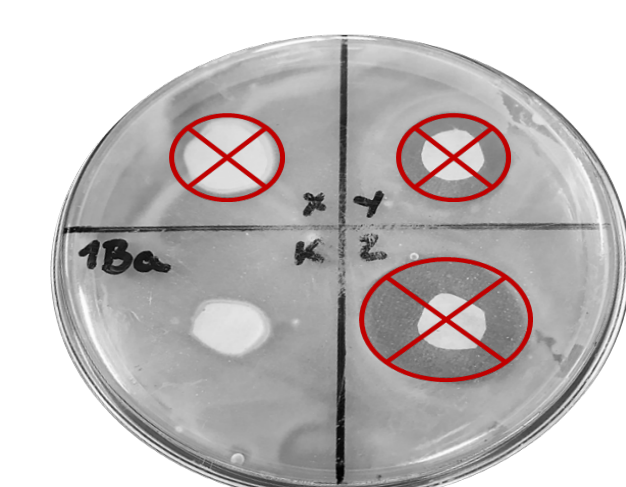


Fig. 2 Inhibition of *E. coli* by oregano oil at concentrations of 32, 64 and 128 μ l/ml.

The biggest inhibition zones were created by essential oils on the bacterium *S. aureus*: 15.5-25.0 mm, less on *M. luteus*: 11.5-23.5 mm and *E. coli*: 13.0-22.5 mm.

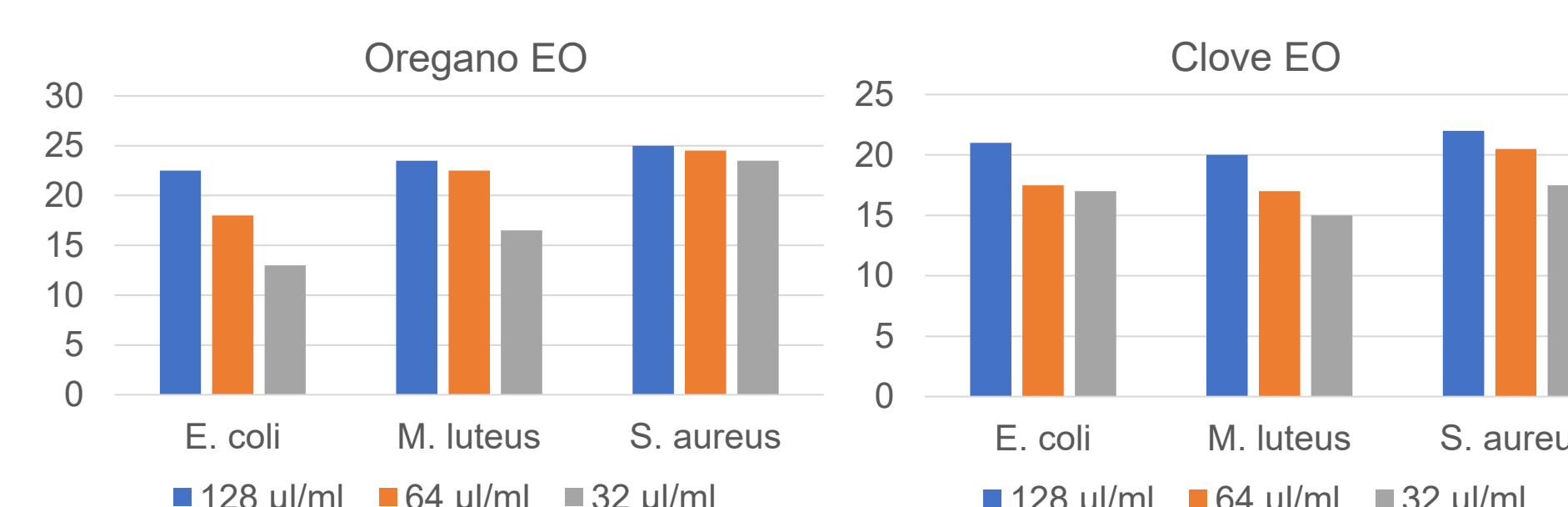


Fig. 3 Inhibition zones [mm] of oregano and clove essential oils

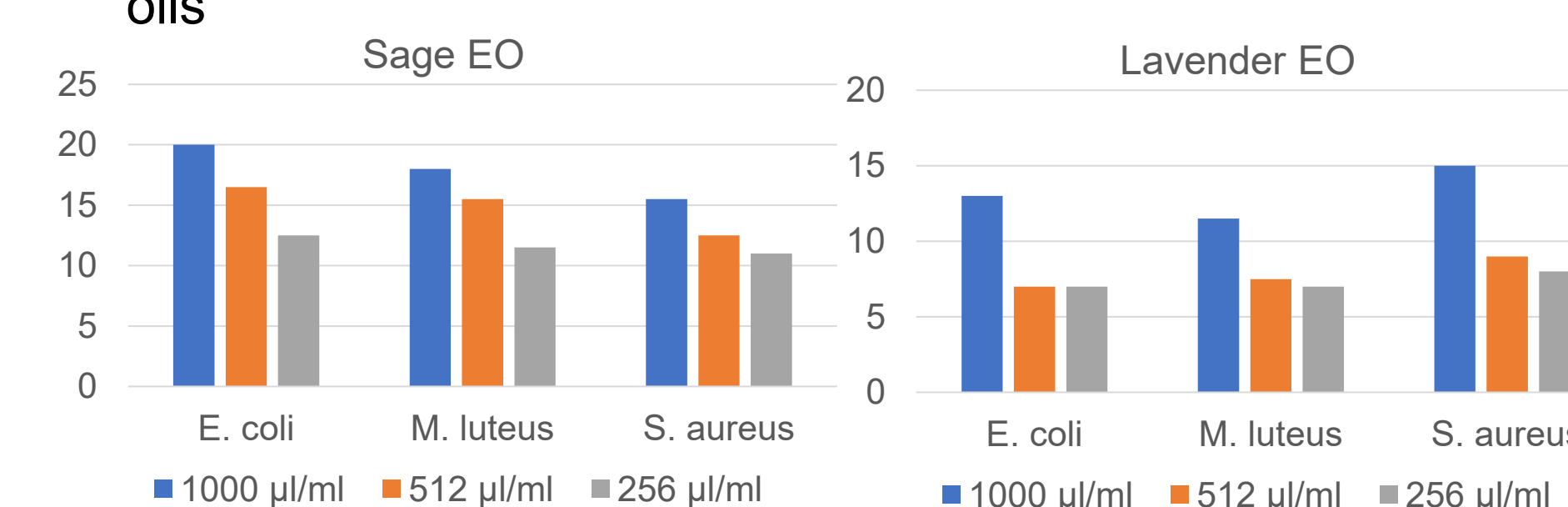


Fig. 4 Inhibition zones [mm] of sage and lavender essential oils

CONCLUSIONS

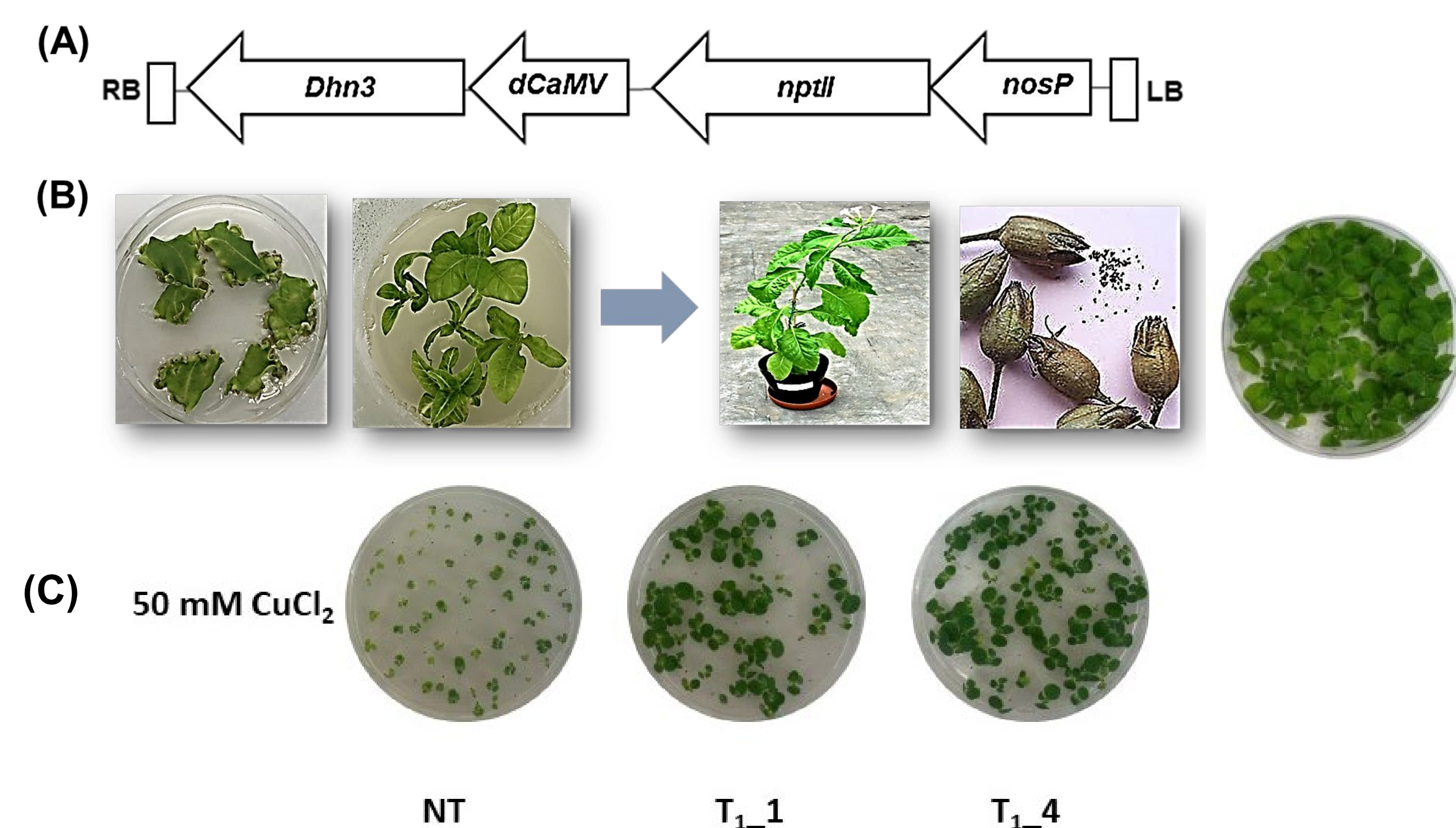
The most significant effects were observed with oregano and clove oil. Lavender oil also had significant antimicrobial potential, as well as sage oil. The most sensitive was the gram-positive bacterium *S. aureus* CCM 4223 with MIC ≤ 1 μ l/ml for all tested essential oils.

Among the tested pure substances, β -caryophyllene caryophyllene oxide and α -humulene showed weak antimicrobial activity.

In our work, we confirmed that essential oils with β -caryophyllene as one component were more effective than pure substances.

ACKNOWLEDGEMENTS

This work was supported by APVV-20-0413 project.



Dehydrins (PF00257) are thermostable and highly hydrophilic proteins that are associated mainly with later stages of plant embryogenesis. Besides that, many studies indicate their role in plant stress tolerance.

The work is aimed to study the effect of an overexpression of the dehydrin gene (Dhn3) from *Quercus robur* L. (AY607707.1) in transgenic tobacco plants on alleviation of copper stress during seed germination.

Transgenic plants overexpressing the gene Dhn3 (**Fig. 1A, B**) were germinated under 50 mM CuCl₂ (**Fig. 1C**) and analysed. The expression of the genes involved in plant antioxidant system (superoxide dismutase SOD, catalase CAT, dehydroascorbate reductase DHAR), defence response (beta-1,3 glucanase GLU), metal transporters (heavy metal ATPases HMA_A and HMA_B, metal transport proteins MTP1_A, MTP1_B) were quantified using qPCR (**Fig. 2**).

Conclusions An overexpression of the gene Dhn3 altered the expression of antioxidant enzymes (SOD, CAT) and PR proteins (GLU), compared to non-transgenic NT seedlings. In non-transgenic (NT) tobacco seedlings, applied stress significantly increased the expression of the genes encoding antioxidant enzymes SOD (4.5 fold), DHAR (4 fold), GLU (2.5 fold), (HMA_A and HMA_B (2 and 2.5 folds), NtMTP1_A, NtMTP1_B (3 and 6 folds); while in stressed (T₁) transgenic seedlings the expression of the genes SOD, DHAR, GLU, NtHMA_A, NtHMA_B, NtMTP1_A, NtMTP1_B did not significantly change, compared to their non-stressed counterparts. An overexpression of the dehydrin Dhn3 in transgenic tobacco plants contributed to the alleviation of copper stress during seed germination.

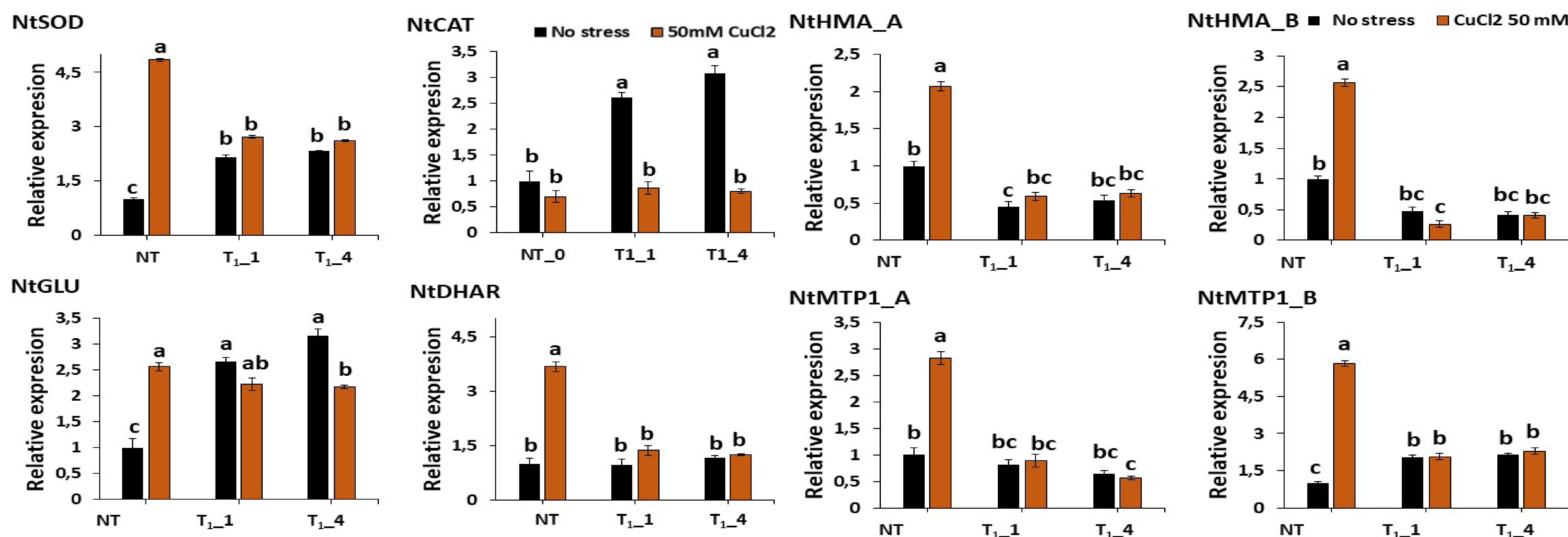


Fig. 2 Relative expression of genes encoding antioxidant enzymes (NtSOD, NtCAT, NtDHAR), PR proteins (NtGLU) and selected metal transporters (NtHMA_A, NtHMA_B, NtMTP1_A, NtMTP1_B) in transgenic and non-transgenic seedlings germinated in the presence of 50 mM CuCl₂. Relative expression levels were normalized to the actin gene. Data are mean ± SE. Letters indicate statistically significant differences at p ≤ 0.05.

TWO NOVEL CLOSELY RELATED SUBFAMILIES OF THE ALPHA-AMYLASE FAMILY GH13

Filip Mareček¹ & Štefan Janeček^{1,2}¹ Laboratory of Protein Evolution, Institute of Molecular Biology, Slovak Academy of Sciences, Bratislava, Slovakia² Institute of Biology and Biotechnology, Faculty of Natural Sciences, University of SS. Cyril and Methodius, Trnava, Slovakia

INTRODUCTION

The CAZy database classifies glycoside hydrolases and other enzyme classes involved in the breakdown, biosynthesis and modification of carbohydrates into so-called families [1]. Enzymes associated with the starch degradation are referred to as amylolytic and α -amylase is an integral part of this process. α -Amylases catalyze endohydrolysis of α -1,4-glucosidic linkages in polysaccharides that consist of at least three α -1,4-linked glucose units [2]. The main α -amylase family GH13 is one of the largest families within the CAZy database [1], covering more than 30 enzyme specificities. Enzymes that are structurally related to α -amylase are represented by the CAZy clan GH-H consisting of three families, i.e., the families GH70 and GH77 in addition to the main family GH13 [2]. At a lower level of the hierarchy, the family GH13 is divided into 47 subfamilies, reflecting the closer sequence and/or specificity relatedness of individual groups of enzymes [3,4,5]. Family GH13 classifies also sequences that, due to their structure-sequence features, have not yet been assigned to any of the established GH13 subfamilies. This is the case of the maltogenic amylase from *Thermotoga neopolitana* [6,7] and the α -amylase from *Haloarcula japonica* [8]. The present study delivers a detailed *in silico* analysis of two mutually related groups of proteins represented by the above-mentioned enzymes to indicate their position in the context of the main α -amylase family GH13.

AIM OF THE STUDY

The main objectives of the presented *in silico* study are to: (i) indicate whether or not are within the main α -amylase family GH13 two related groups of enzymes that are worthy of creating new official subfamilies within the CAZy database. The first group could be represented by the α -amylase from *Haloarcula japonica*, while the latter one by maltogenic amylase from *Thermotoga neopolitana*; (ii) identify sequence-structural features of these two groups of enzymes and hypothetical proteins that could clearly demonstrate their mutual evolutionary relatedness, but on the other hand, confirm that these two groups represent two independent subfamilies of the main α -amylase family GH13.

MGA from *Thermotoga neopolitana* (4GKL [7]; blue group) "AAMY" from *Lactopantibacillus plantarum* (3DHU, unpublished; blue group)

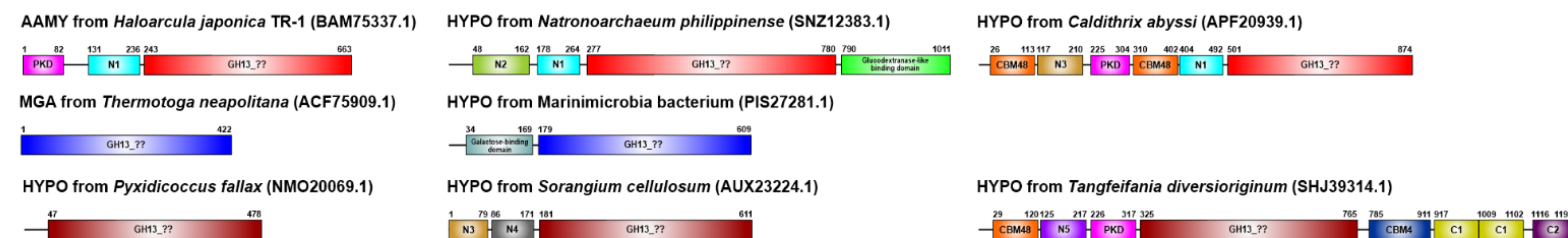
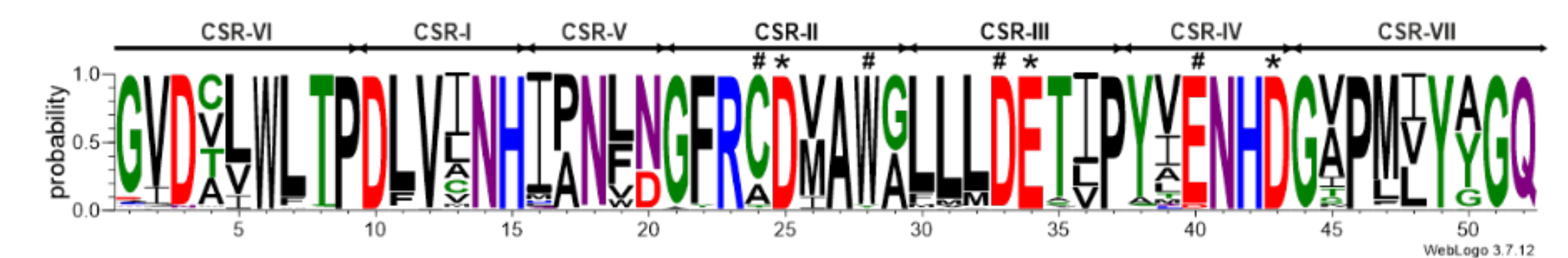
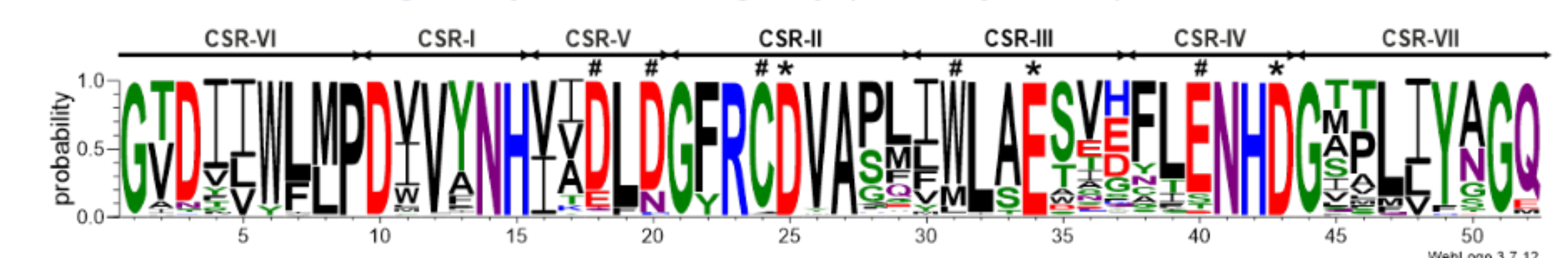


Figure 1. Domain arrangement of selected representatives of the study. The eight representatives were chosen to best represent the situation within the two novel closely related GH13 subfamilies (first two rows) as well as in the intermediary group (last row). The individual domains are colored as follows: catalytic domain - red/blue/burgundy (depending on the group to which the enzyme or hypothetical protein belongs); Polycystic kidney disease domain (PKD) - magenta; N1 - cyan; N2 - marian green; N3 - gold; N4 - grey; N5 - purple; C1 - yellow-green; C2 - plum; CBM48 - orange; CBM4 - navy blue; glucodextranase-like binding domain - grey-green.

AAMY from *Haloarcula japonica* TR-1-like group (386 sequences)



MGA from *Thermotoga neopolitana*-like group (280 sequences)



Intermediary group (26 sequences)

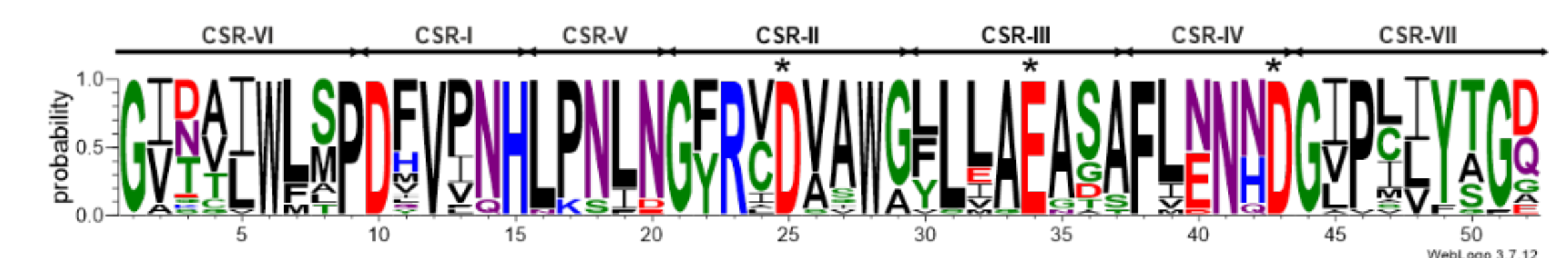


Figure 2. Sequence logos of the seven well-established GH13 CSRs of three following groups (in accordance with the evolutionary tree): (a) Group represented by the α -amylase from *Haloarcula japonica* (red; 386 sequences); (b) Group represented by the maltogenic amylase from *Thermotoga neopolitana* (blue; 280 sequences); (c) Group represented by the hypothetical protein from *Sorangium cellulosum* (burgundy; 26 sequences). CSR-I, residues 10-15; CSR-II, residues 23-31; CSR-III, residues 32-39; CSR-IV, residues 40-45; CSR-V, residues 16-20; CSR-VI, residues 1-9; CSR-VII, residues 46-54. The catalytic triad, i.e. the catalytic nucleophile (No. 25, aspartic acid), the proton donor (No. 34, glutamic acid) and the transition-state stabiliser (No. 43, aspartic acid) are indicated by asterisks. The well-conserved residues, which could represent specific features of the two novel GH13 subfamilies identified by the analysis are indicated by hashtag.

CONCLUSIONS

(1) The presented study delivers a detailed *in silico* analysis of 692 sequences from two closely related groups of GH13 enzymes and hypothetical proteins. The first group could be represented by the α -amylase from *Haloarcula japonica*, while the latter one by maltogenic amylase from *Thermotoga neopolitana* (Fig. 1).

(2) Comparison of amino acid sequences of the aforementioned two related groups of enzymes and hypothetical proteins was focused mainly on 7 well-established CSRs of the family GH13. Both of the groups share some common sequence features e.g. well-conserved cysteine before the catalytic nucleophile (Fig. 2; position 24); or well-conserved glutamic acid in the CSR-IV (Fig. 2; position 40), but at the same time also bearing their own characteristics (Fig. 2).

(3) The maximum-likelihood evolutionary tree of the whole family GH13 (Fig. 3) was calculated based on a substantial stretch of the catalytic domain extending from the β 2 strand up to the β 8 strand i.e. the segment covering all seven CSRs. Phylogenetic analysis supports the hypothesis that the two above-mentioned groups represent two related but at the same time independent GH13 subfamilies. Moreover, results suggest that the representatives of α -glucosidases from the subfamily GH13_38 are most closely related to the novel subfamilies (Fig. 3).

(4) Structural analysis of the maltogenic amylase from *Thermotoga neopolitana* with the 3D structures/models of selected representatives of the study revealed the highest degree of similarity with the 3D structure of " α -amylase" from *Lactopantibacillus plantarum* (Fig. 4). The 3D structure of this enzyme was solved in 2008, and the enzyme was without further biochemical characterization designated as an α -amylase. Nevertheless, our analysis indicated the conservation of important non-reducing end sugar-binding site residue - D135 (MGA from *T. neopolitana*) in the structure of " α -amylase" from *Lactopantibacillus plantarum* (Fig. 4). This suggests possible similar mode of action of these enzymes.

References

- [1] Drula V., Garron M.L., Dogan S., Lombard V., Henrissat B. & Terrapon N. (2022) *Nucleic Acids Res.* 50: D571–D577.
- [2] Janeček S., Svensson B. & MacGregor E.A. (2014) *Cell. Mol. Life Sci.* 71: 1149–1170.
- [3] Stam M.R., Danchin E.G., Rancurel C., Coutinho P.M. & Henrissat B. (2006) *Protein Eng. Des. Sel.* 19: 555–562.
- [4] Janeček S. & Svensson B. (2022) *Amylase* 6: 1–10.
- [5] Mareček F. & Janeček S. (2022) *Molecules* 27: 8735.
- [6] Park K.-M., Jun S.-Y., Choi K.-H., Park K.-H., Park C.-S. & Cha J. (2013) *Appl. Microbiol. Biotechnol.* 86: 555–566.
- [7] Jun S.-Y., Kim J.-S., Choi K.-H., Cha J. & Ha N.-C. (2010) *Acta Crystallogr.* D69: 442–450.
- [8] Onodera M., Matsunami R., Tsukimura W., Fukui T., Nakasone K., Takashina T., & Nakamura S. (2013) *Biosci. Biotechnol. Biochem.* 77: 281–288.

Acknowledgement. This work was financially supported by the Grant 2/0148/21 from the Slovak Grant Agency VEGA.

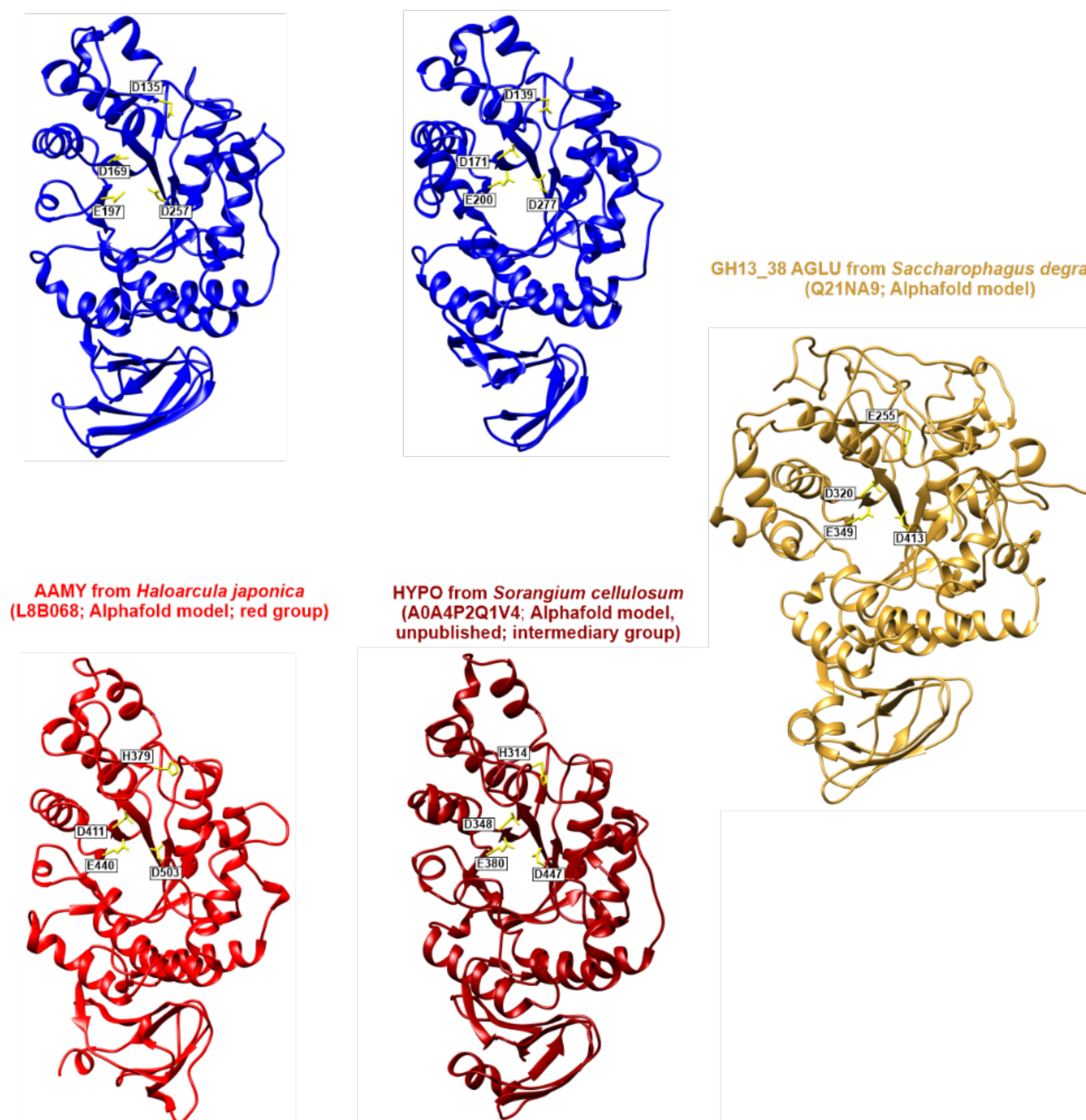


Figure 4. 3D structures and AlphaFold models of the 3D structures of the selected representatives of the study Side chains of the catalytic residues or predicted catalytic residues, respectively are displayed (yellow). The residue that is involved in non-reducing end sugar-binding site of the MGA from *T. neopolitana* - D135 and corresponding residues in other structures/models are also shown. The models were obtained by the DeepMind software AlphaFold (<https://alphafold.ebi.ac.uk/>).

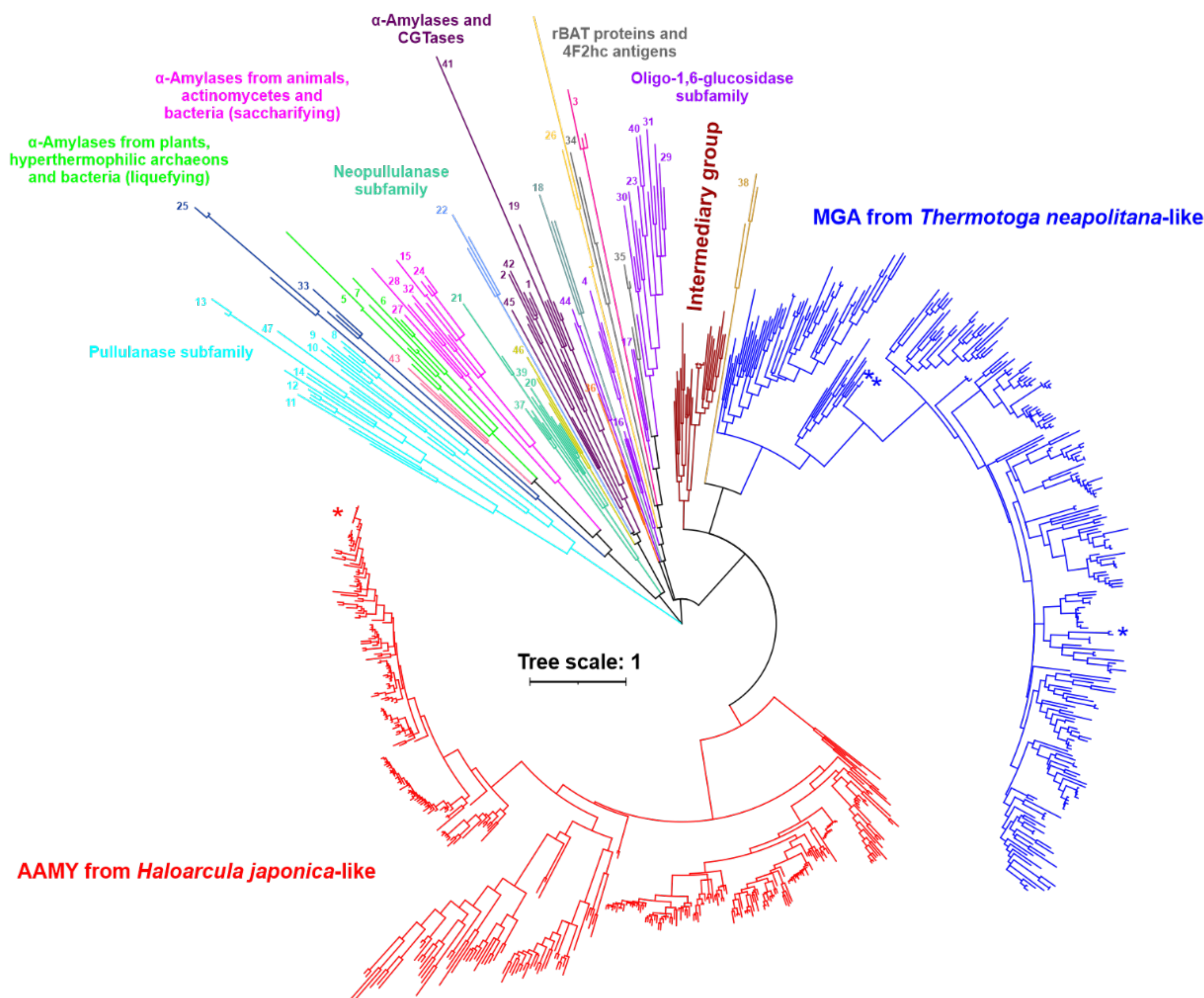


Figure 3. Evolutionary tree of the main α -amylase family GH13 with two novel closely related subfamilies. The tree covers 833 sequences with a focus on the novel subfamilies around the α -amylase from *Haloarcula japonica* and maltogenic amylase from *Thermotoga neopolitana*, respectively. The tree is based on the alignment, spanning the sequence segment from the beginning of the strand β 2 (CSR-VI) to the end of the strand β 8 (CSR-VII), i.e. the substantial part of the catalytic TIM-barrel including the domain B. For the sake of simplicity, only the branches leading to the individual GH13 subfamilies, marked by their numbers, are shown. Characterized members of the individual groups are labeled by an asterisk.



ANS 2023

The expression level of the CysPC domain of mitochondrial calpain in W10BSmL white mutant compared to wild type *Euglena gracilis* strain Z

Dominika Vešelényiová, Juraj Krajčovič, Zuzana Gerši

University of Ss. Cyril and Methodius in Trnava, Faculty of Natural Sciences, Nám. J. Herdu 2, 917 01 Trnava, Slovak Republic

INTRODUCTION

- Calpains (EC 3.4.22.17), calcium-activated cysteine proteases participate in many cellular processes and are well-characterised in many animals and plants, but not in the protist (taxon Euglenida).
- The mitochondrion of *Euglena gracilis* is a single, large and reticulated organelle, a trait that is by no means unique among protists. Recently, the sequence of mitochondrial calpain was identified in the transcriptome of *E. gracilis* using *in silico* methods.
- Mitochondrial calpain consists of conservative CysPC and Calpain III domain.

AIM

To detect and compare the gene expression level of mitochondrial calpain of the wild-type *E. gracilis* and its stable bleached mutant W10BSmL.

MATERIALS AND METHODS

- Cell cultures of wild-type *Euglena gracilis* strain Z (EgZ) and *E. gracilis* W10BSmL (W10) white mutant grown in CM medium for 24 h at light and a temperature of 23 °C.

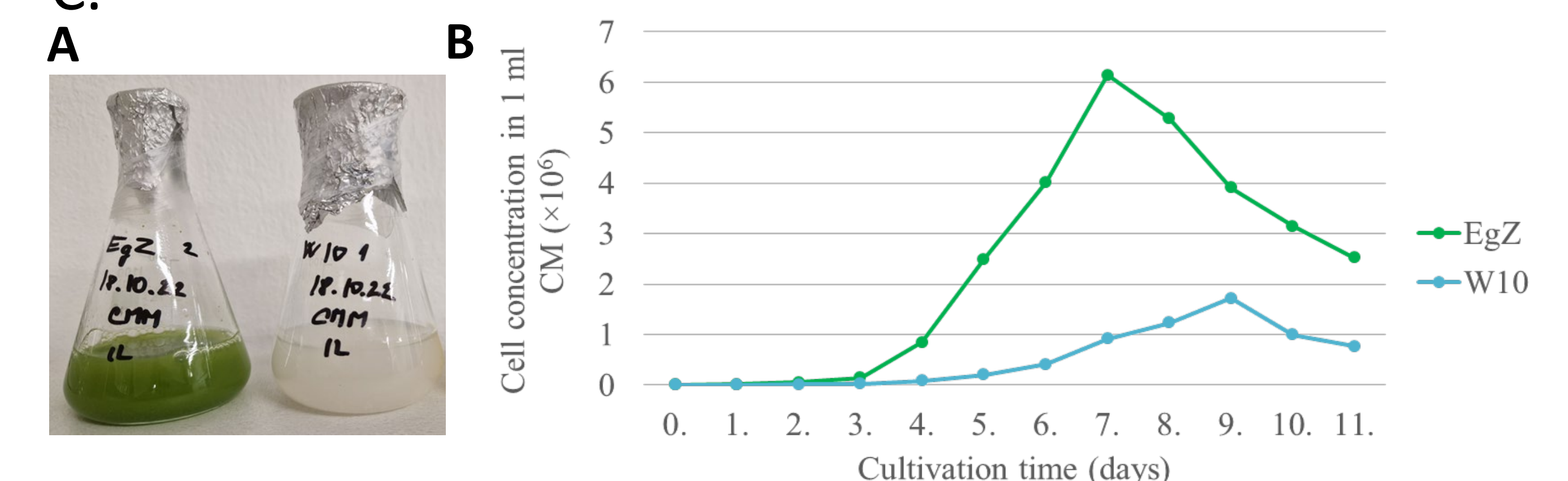


Fig. 1. A - cell cultures of *Euglena gracilis* strain Z (left) and W10BSmL mutant (right) in CM medium after 10 day of cultivation. B - Growth profiles of EgZ and W10 cells.

- The expression comparison of mutant W10BSmL and *E. gracilis* wild-type revealed significant differences.
- The analysis showed higher (2,57 times) expression of selected mitochondrial gene in W10BSmL in comparison with wild-type cells.

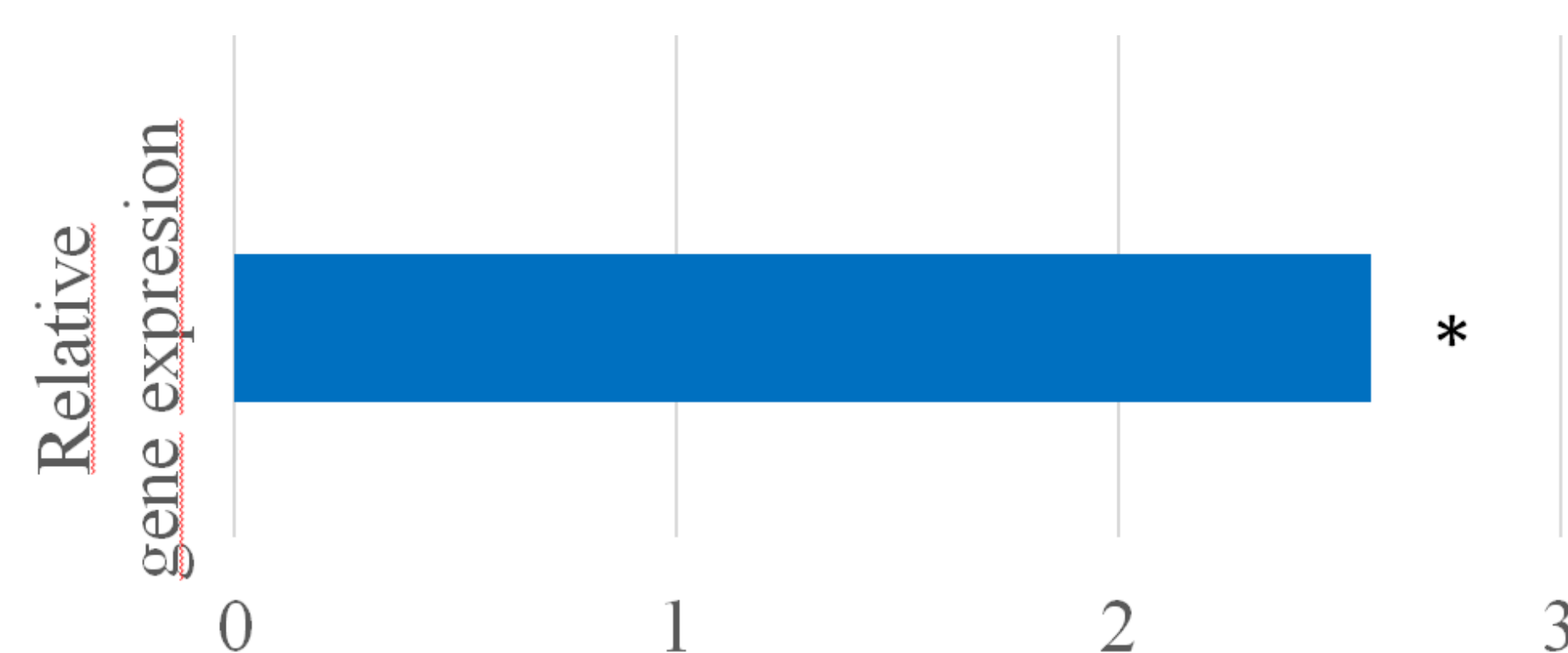


Fig. 2. Relative expression of the CysPC domain of mitochondrial calpain gene (eugra1980.p1.) in white mutant W10BSmL of *Euglena gracilis*. Expression level was analyzed by RT-qPCR and normalized over the *cox1* gene.

RESULTS

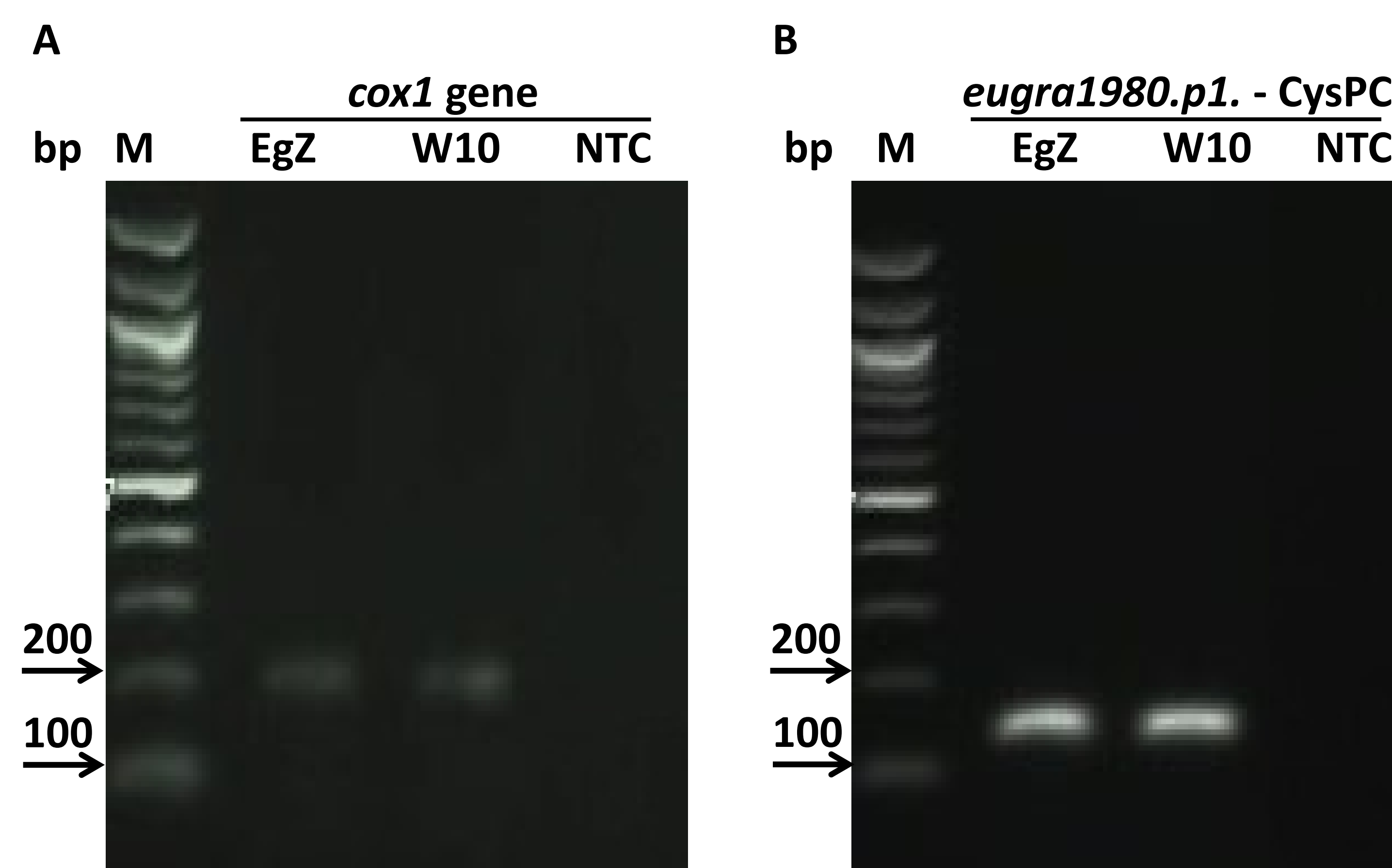


Fig. 3. Amplification of 191 bp DNA fragment of reference gene (*cox1*) (A) and 142 bp DNA fragment of the mitochondrial calpain gene (CysPC domain of eugra1980.p1) (B) detected by RT-qPCR in *Euglena gracilis* strain Z and W10BSmL bleached mutant. NTC – negative control.

- cDNA was prepared by reverse transcription from total RNA
- Using quantitative RT-PCR analysis was amplified a segment of the CysPC domain of the mitochondrial calpain and *cox1* gene (reference gene).
- The relative expression was interpreted according to the Livak method.

CONCLUSIONS

The activity of the mitochondrial calpain gene is 2.5 times higher in the white mutant W10BSmL.

ACKNOWLEDGEMENTS

This work was supported by the grant VEGA 1/0694/21.

Preparation of the plant extracts with significant enhanced bio-activity, by application of innovative engine, worked on simultaneous application of several physical factors for new food supplements generation.

TIBOR MALIAR^{1*}, MARCELA BLAŽKOVÁ^{1,2}, MAREK KUNŠTEK^{1,2}, MÁRIA MALIAROVÁ¹

¹Department of Chemistry, Faculty of Natural Sciences, University of Ss. Cyril and Methodius in Trnava, Námestie. J. Herdu 2, 917 01 Trnava, Slovak Republic.

²National Agricultural and Food Centre, Hlohovecká 2, 951 41 Lužianky, Slovak Republic.

ABSTRACT

It has been developed original engine for frugal extraction of plant extractive compounds with accelerating effect, worked upon the principle of the simultaneous combination of several physical factors (sonication, temperature, by electrical field promoting extraction device). By application of this engine, it was obtained plant extract samples with several times enhanced dry matter content as well as bio-activity, particularly antioxidant activity, antibacterial activity, inhibition activity on pathophysiological important enzymes, anti-inflammatory activity etc. This device was utilized in the process of the extract samples preparation. Several prepared samples expressed significant simultaneous antibacterial effect, inhibition activity on Main protease of SARS-CoV-2, antioxidant activity as well as anti-inflammatory activity. Especially extract samples from bark of oak (*Quercus robur*, L.), silver birch (*Betula pendula*, L.) or leaves of horse chestnut (*Aesculus hippocastanum*, L.) and others. The enhancement factor (coefficient) varied in interval (2,8 - 6,2). The extraction products were prepared for development of new food supplements for pandemic situation, aimed to enhance defensiveness of human body.

INTRODUCTION

The necessity of bio-active compounds as perspective drugs or agents with preventive/therapeutic effect for food supplements it is really evident [1]. The basic screening of bio-activity of compounds/medical plant extracts consist of several basic assays – for antioxidant activity, anti-microbial activity, anti-inflammatory activity and basic enzyme inhibition activity included anti-proteinase activity [2]. In this authors team is currently studied modern and perspective determination of antioxidant/pro-oxidant activity in simultaneous tests on one microplate [3, 4]. The commercial database Scifinder, one of the most widely utilized databases, reveals a significant lack of scientific papers about pro-oxidants, especially papers describing the results of simultaneously tested antioxidant/pro-oxidant activity. Previous COVID pandemic period created a focus on papers about perspective entities with antiviral activity (especially SARS-CoV-2 3CLproteinase inhibitors) antibacterial activity and anti-inflammatory activity [5 - 7]. The bioactivity enhancement of medical plant extracts could be carried out beside reactive extraction or by realized by physical treatment [8 - 10] .

1. Henry Ivan A. Boy et al. Recommended Medicinal Plants as Source of Natural Products: A Review. *Digital Chinese Medicine*, 1(2): 131-142, 2018.
2. Miryam Amigo-Benavent et al. Chapter 6 - Methodologies for bioactivity assay: biochemical study. *Biologically Active Peptides, From Basic Science to Applications for Human Health*, 2021, Pages 103-153.
3. Prieto, M. A. et al. p-Carotene Assay Revisited. Application To Characterize and Quantify Antioxidant and pro-oxidant Activities in a Microplate. *Journal of Agricultural and Food Chemistry*, 60 (36), 8983-8993, 2012.
4. Prieto, M.A. et al. Crocin bleaching antioxidant assay revisited: Application to microplate to analyse antioxidant and pro-oxidant activities. *Food Chemistry*, 167, 299-310, 2015.
5. Cheorl-Ho Kim. Anti-SARS-CoV-2 Natural Products as Potentially Therapeutic Agents. *Frontiers in pharmacology*, 12, article 590509, 2021.
6. François Chassagne et al. A Systematic Review of Plants With Antibacterial Activities: A Taxonomic and Phylogenetic Perspective. *Frontiers in pharmacology*, 11, article 586548, 2011.
7. Mabozou Kpemiissi et al. Anti-cholinesterase, anti-inflammatory and antioxidant properties of *Combretum micranthum* G. Don: Potential implications in neurodegenerative disease. *IBRO Neuroscience Reports*, 14, 21-27, 2023.
8. Wan Zuhairi Saad et al. Effects of Heat Treatment on Total Phenolic Contents, Antioxidant and Anti-Inflammatory Activities of *Pleurotus sajor-caju* Extract. *International Journal of Food Properties*, 17:219-225, 2014.
9. Meirlielly S. Jesusa et al. Ohmic heating polyphenolic extracts from vine pruning residue with enhanced biological activity. *Food Chemistry*, 316, 126298, 2020.
10. E. Conde et al. Antioxidant activity of the phenolic compounds released by hydrothermal treatments of olive tree pruning. *Food Chemistry*, 114, 806-812, 2009.

MATERIALS AND METHODS

- The original engine for frugal extraction of plant extractive compounds with accelerating effect consist of following applications: heating by AC electrode heating, fixed in non-conductor wall of engine, equipped by ultrasonic moduli, either stirrer device, with the possibility of air evaporation (oxygen removing). This engine is equipped for normal/reactive extraction promoted by heating, AC electric field and sonication.
- The subject of extraction it is dried medical plant matter, fragment to pieces less than 5 mm in diameter, suspended in distilled water or water/ethanol mixture in ration 9:1 to 1:1.
- Antiviral activity of the extracts was expressed as inhibition activity on main 3CLproteinase of SARS-CoV-2 virus, determined by adapted method using gold nano-particles, derivatized by pentaoligopeptide H₂N-EEEEESAVLQSGFRC-COOH, the releasing of gold nanoparticles aggregation blocking is measured by significant color increasing at 630 nm, output parameter is IC₅₀ value expressed in mg of dried matter/ml.
- Anti-inflammatory activity was determined on PMA stimulated leucocytes, isolated from peripheral blood of lab animal, measured as fluorescence detection of radical production in percentual expression.
- Antibacterial activity was tested on following bacterial strains: (carbapenemase producing *Klebsiella ssp.*, ESBL *Enterococcus aerogenes*, MDR *Pseudomonas aeruginosa* and *Acinetobacter baumannii*, VRE *Enterococcus faecium* and MRSA *Staphylococcus aureus*) on microplates using convenient dilution mode in MHB, output parameter is MIC expressed in mg of dried matter /ml.
- Antioxidant activity was measured by scavenging of model DPPH[•] radical, measured as decrease at 520 nm, output parameter is IC₅₀ value expressed in mg of dried matter per milliliter.
- Pro-oxidant activity was measured by percentual measure of ion Fe³⁺ conversion to more pro-oxidant Fe²⁺ ion, measured as increase at 630 nm, output parameter is IC₅₀ value expressed in mg of dried matter /ml.

RESULTS

The scheme of constructed engine is presented on following Figure 1.

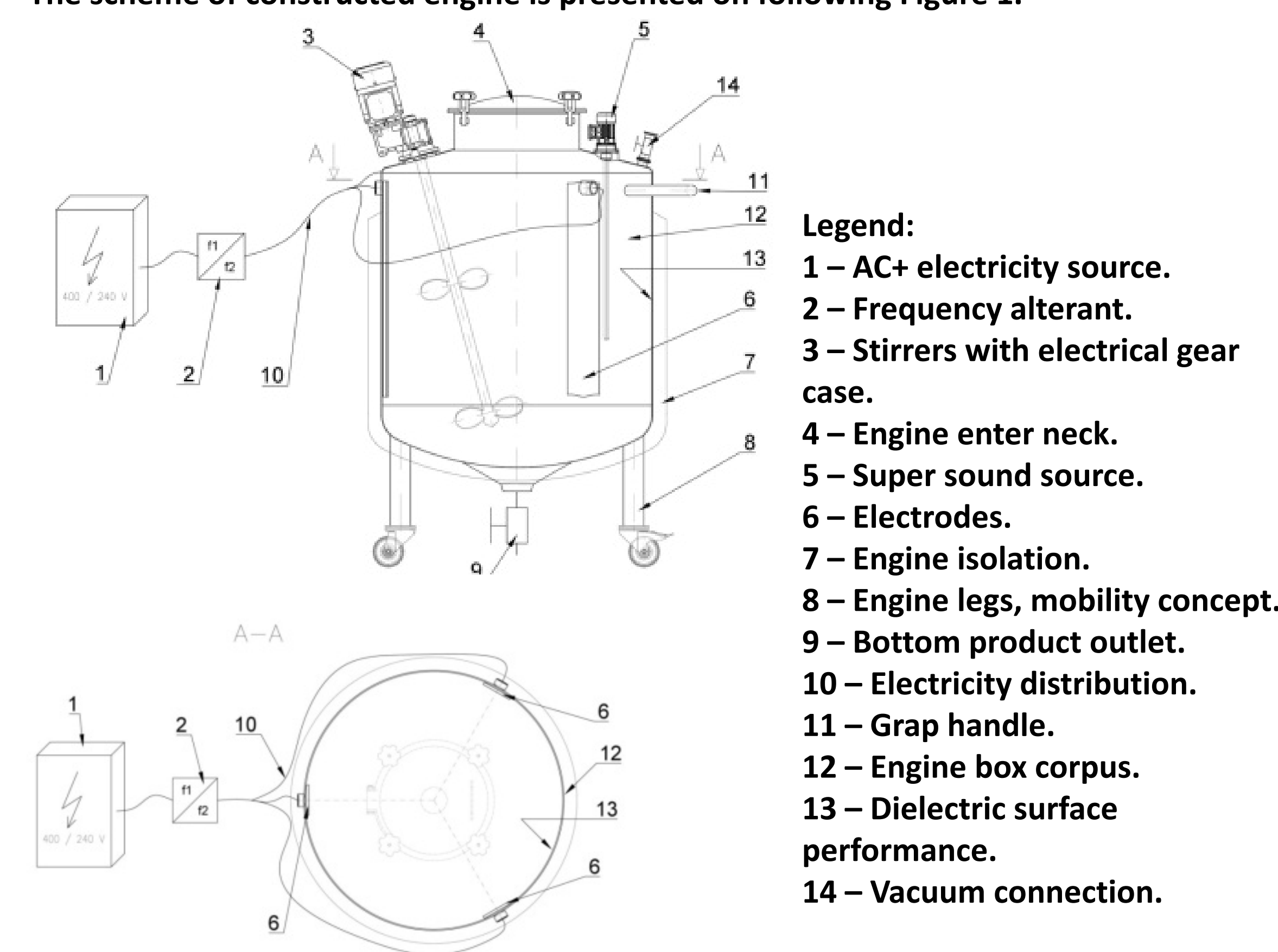


Figure 1. The scheme of constructed engine.

The example of the best results with enhanced extractivity, expressed as increasing of dried matter of extracts, as well as enhancing of bioactivity, expressed by enhancing factor for chosen medical plant matter /extracts/ is presented in Table 1.

Table 1. The increasing of extractivity, bioactivity for selected (medical) plant extracts, expressed as Enhancement Factor /EF/.

Dried matter of plant	EF for /DM/ (dried matter) in extracts	EF for /AVA/ Inhibition of 3CLpro SARS-Cov-2	EF for /AFA/ Inhibition of PMA stimulated leucocytes	EF for /AOXA/ scavenging of DPPH [•] radical	EF for /PROXA/ the measure of conversion of Fe ³⁺ to Fe ²⁺	EF for /ABA/ MIC _{AVG} on 8 bacterial strains
Oregano, <i>Origanum vulgare</i> , flower	3,1	3,1	3,5	5,1	4,5	3,6
Sessile oak, <i>Quercus petraea</i> , bark	4,2	4,3	4,4	6,0	6,2	4,3
Rapeseed, <i>Brassica napus</i> , grains	2,8	3,1	3,0	4,0	4,5	3,6
Oat, <i>Avena sativa</i> , grains	2,9	3,5	3,5	4,5	5,0	3,9

CONCLUSIONS

1. The natural extracts are still a very perspective subject of the research, aimed to discover and offer new skeletal types for drug generations.
2. Currently there are interesting a plant extracts with dual/multimodal therapeutic potency, in this paper are desired medical plant extracts with simultaneous antioxidant, antibacterial, antiviral and anti-inflammatory activity.
3. Flower extract of oregano, *Origanum vulgare*, bark extract of sessile oak, *Quercus petraea*, and grain extract of rapeseed, *Brassica napus* and oat, *Avena sativa* were selected for their multimodal bioactivity effect.
4. Mentioned extract were subjected to the study of enhancement of bioactivity by the original engine, able to realize frugal extraction of plant extractive compounds with accelerating effect.
5. The value of dry matter in extracts was increased by factor 2,8 – 4,2; antiviral activity measured by inhibition of 3CLpro SARS-Cov-2 by factor 3,1 – 4,3; anti-inflammatory activity, measured as suppression of PMA stimulated leucocytes by factor 3,0 – 4,4; antioxidant activity measured by scavenging of model DPPH[•] radical by factor 4,0 – 6,0; pro-oxidant activity measured as degree of conversion Fe³⁺ to Fe²⁺ by factor 4,0 -6,2 and finally antibacterial activity by factor 3,6 -4,3.
6. Simultaneous effect of temperature, ultrasonic, extract promotion by electric field under oxygen content low conditions leads to increase desiring bioactivity by factor 3 – 6,2.
7. The next future HPLC analysis would reveal if the content of the extraction sample is different, thus if the extraction accelerating factors promote the extraction of the same or different compounds.
8. The medical plant extracts prepared by describing methodology are very perspective for new food supplements generation.

ACKNOWLEDGEMENTS

This paper was supported by grant No. SRDA-20-0413.